



## RESEARCH ARTICLE

10.1002/2015JG003083

## Key Points:

- Wetland energy and carbon fluxes varied seasonally and between study periods
- Standing dead plant material may have reduced overall wetland productivity
- Large measured methane emissions offset the radiative cooling from photosynthetic carbon uptake

## Supporting Information:

- Supporting Information S1

## Correspondence to:

F. E. Anderson,  
fanders@usgs.gov

## Citation:

Anderson, F. E., et al. (2016), Variation of energy and carbon fluxes from a restored temperate freshwater wetland and implications for carbon market verification protocols, *J. Geophys. Res. Biogeosci.*, 121, doi:10.1002/2015JG003083.

Received 5 JUN 2015

Accepted 10 FEB 2016

Accepted article online 16 FEB 2016

## Variation of energy and carbon fluxes from a restored temperate freshwater wetland and implications for carbon market verification protocols

Frank E. Anderson<sup>1</sup>, Brian Bergamaschi<sup>1</sup>, Cove Sturtevant<sup>2</sup>, Sara Knox<sup>2</sup>, Lauren Hastings<sup>3</sup>, Lisamarie Windham-Myers<sup>4</sup>, Matteo Dettò<sup>5</sup>, Erin L. Hestir<sup>6</sup>, Judith Drexler<sup>1</sup>, Robin L. Miller<sup>1</sup>, Jaclyn Hatala Matthes<sup>2</sup>, Joseph Verfaillie<sup>2</sup>, Dennis Baldocchi<sup>2</sup>, Richard L. Snyder<sup>7</sup>, and Roger Fujii<sup>1</sup>

<sup>1</sup>U.S. Geological Survey, Sacramento, California, USA, <sup>2</sup>Ecosystem Science Division, Department of Environmental Science, Policy and Management, University of California, Berkeley, California, USA, <sup>3</sup>Delta Stewardship Council, Sacramento, California, USA, <sup>4</sup>U.S. Geological Survey, Menlo Park, California, USA, <sup>5</sup>Smithsonian Tropical Research Institute, Panama City, Panama, <sup>6</sup>Department of Marine, Earth and Atmospheric Sciences, North Carolina State University, Raleigh, North Carolina, USA, <sup>7</sup>Department of Land, Air and Water Resources, University of California, Davis, California, USA

**Abstract** Temperate freshwater wetlands are among the most productive terrestrial ecosystems, stimulating interest in using restored wetlands as biological carbon sequestration projects for greenhouse gas reduction programs. In this study, we used the eddy covariance technique to measure surface energy carbon fluxes from a constructed, impounded freshwater wetland during two annual periods that were 8 years apart: 2002–2003 and 2010–2011. During 2010–2011, we measured methane ( $\text{CH}_4$ ) fluxes to quantify the annual atmospheric carbon mass balance and its concomitant influence on global warming potential (GWP). Peak growing season fluxes of latent heat and carbon dioxide ( $\text{CO}_2$ ) were greater in 2002–2003 compared to 2010–2011. In 2002, the daily net ecosystem exchange reached as low as  $-10.6 \text{ g C m}^{-2} \text{ d}^{-1}$ , which was greater than 3 times the magnitude observed in 2010 ( $-2.9 \text{ g C m}^{-2} \text{ d}^{-1}$ ).  $\text{CH}_4$  fluxes during 2010–2011 were positive throughout the year and followed a strong seasonal pattern, ranging from  $38.1 \text{ mg C m}^{-2} \text{ d}^{-1}$  in the winter to  $375.9 \text{ mg C m}^{-2} \text{ d}^{-1}$  during the summer. The results of this study suggest that the wetland had reduced gross ecosystem productivity in 2010–2011, likely due to the increase in dead plant biomass (standing litter) that inhibited the generation of new vegetation growth. In 2010–2011, there was a net positive GWP ( $675.3 \text{ g C m}^{-2} \text{ yr}^{-1}$ ), and when these values are evaluated as a sustained flux, the wetland will not reach radiative balance even after 500 years.

### 1. Introduction

Wetlands can be a more effective carbon sink than upland terrestrial ecosystems, as marsh vegetation typically has high gross primary productivity [Rocha and Goulden, 2009] and flooded environments create anaerobic soil conditions that prevent the decomposition of dead biomass and preserve sequestered carbon within the soil profile [Mitra et al., 2005; Savage and Davidson, 2001]. Recently, Mitsch et al. [2013] calculated that wetlands globally have the potential to sequester  $1280 \text{ Tg C yr}^{-1}$  of carbon dioxide ( $\text{CO}_2$ ) from the atmosphere. The preservation and reestablishment of wetlands in subtropical and temperate latitudes could support a large portion of this potential [Aselmänn and Crutzen, 1989], as longer growing seasons lead to greater  $\text{CO}_2$  uptake [Whiting and Chanton, 2001] and suitable conditions exist to favor high phytomass production [Rocha and Goulden, 2009]. However, as much as  $448 \text{ Tg C yr}^{-1}$  of the  $\text{CO}_2$  sequestered may return to the atmosphere as methane ( $\text{CH}_4$ ) [Mitsch et al., 2013]. The anaerobic conditions that promote  $\text{CO}_2$  sequestration also make wetlands the largest natural source of  $\text{CH}_4$  emissions to the atmosphere [Bloom et al., 2010].

While there is good evidence for long-term net carbon accumulation in wetlands over hundreds to thousands of years [Drexler et al., 2009a; Richardson, 2010; Rippke et al., 2010], more research is needed to quantify the short-term carbon balance. Observed interannual variability in wetland net ecosystem exchange (NEE) of  $\text{CO}_2$  has been frequently associated with changes in environmental conditions such as hydro-period, water table depth, the timing and magnitude of precipitation, and air and water temperatures [Bubier et al., 2003; Chu et al., 2014; Lafleur et al., 2003; Petrescu et al., 2015; Roulet et al., 2007]. Although interannual NEE variability may be high, restored wetlands can successfully sequester carbon [Badiou et al., 2011; Knox et al., 2015; Mitsch et al., 2013; Waddington et al., 2010]. As an example, converting agricultural land use to prairie wetlands in the central United States stored  $378 \text{ Tg}$  of organic carbon in the soil and plant biomass,

©2016. The Authors.

This is an open access article under the terms of the Creative Commons Attribution-NonCommercial-NoDerivs License, which permits use and distribution in any medium, provided the original work is properly cited, the use is non-commercial and no modifications or adaptations are made.

as well as through sediment accumulation, within 10 years of establishment [Euliss *et al.*, 2006]. However, there are only a few examples in the literature that document long-term changes in developing freshwater wetland NEE at the decadal time scale [cf. Drexler *et al.*, 2009a; Rocha and Goulden, 2008; Roulet *et al.*, 2007].

Wetland restoration can also provide many other ecosystem services including the reduction of CO<sub>2</sub> respiration from historic soil carbon pools, land surface accretion, and relieving hydrostatic pressure on flood control infrastructure thus improving flood protection, particularly in coastal regions facing accelerated rates of sea level rise [Hatala *et al.*, 2012; Knox *et al.*, 2015; Miller *et al.*, 2008]. Additionally, there is a growing need to better characterize the carbon and global warming potential (GWP) balance of restored wetlands as they may qualify as credited projects in carbon offset programs [e.g., Emmet-Maddox *et al.*, 2010]. To support acceptance of wetland restoration as a creditable means of carbon sequestration, protocols for verification have been adopted or are under consideration by major carbon registries, e.g., Climate Action Reserve, American Carbon Registry, Verified Carbon Standard, and the European Union Emissions Trading System. However, due to the high, short-term variability in wetland NEE versus long-term sequestration, considerable uncertainty exists regarding the efficacy and permanence of such restoration projects and the ability to document any GWP reduction using verification protocols over the 50–100 year period of carbon offset trading programs [Bonn *et al.*, 2014].

Verification protocols also need to consider the effects that CH<sub>4</sub> emissions have on the GWP balance in freshwater wetlands [e.g., Bridgman *et al.*, 2006], as high CH<sub>4</sub> emissions can be relatively consistent despite changes in concurrent CO<sub>2</sub> uptake [Chu *et al.*, 2015]. Modeled estimates of global CH<sub>4</sub> emissions from wetlands range from 60 to 210 Tg C yr<sup>-1</sup> [Bloom *et al.*, 2010; Bridgman *et al.*, 2013], corresponding to a range from 2.0 to 7.1 Pg C yr<sup>-1</sup> (CO<sub>2</sub>-equivalent), given the GWP of CH<sub>4</sub> is 34 times CO<sub>2</sub> for a 100 year time horizon [Myhre *et al.*, 2013]. Even though CH<sub>4</sub> emitted by wetlands may be only a small fraction (1.3 Pg C yr<sup>-1</sup>, globally) of the CO<sub>2</sub> sequestered [Mitsch *et al.*, 2013], the CO<sub>2</sub> equivalent of CH<sub>4</sub> emission rates has shown to be greater than CO<sub>2</sub> storage rates in wetland systems over short time horizons [Petrescu *et al.*, 2015; Whiting and Chanton, 2001]. For restoration projects this can become significant as it may take decades to centuries for restored wetland radiative forcing to become negative [Neubauer, 2014; Petrescu *et al.*, 2015], time in which changes in CO<sub>2</sub> uptake could alter the creditable sequestration benefit. Furthermore, Neubauer and Megonigal [2015] make a compelling argument that wetlands should be treated as a continuous source of methane, suggesting that the creditable benefit would be lower at market-relevant time scales.

In this study, we present the ecosystem exchange of atmospheric CO<sub>2</sub> and CH<sub>4</sub> data from different successional stages of a restored wetland, thus illustrating an 8 year interval of change for consideration in the development of monitoring and verification protocols within carbon emissions offset programs. Our study site is situated in the temperate climate of the western Sacramento-San Joaquin Delta, California, USA. Once an expansive, freshwater tidal marsh system, it was reclaimed for agriculture beginning in 1869 [Thompson, 1957]. In 1997, 7 ha of freshwater wetlands were restored on historical peat soils to test the potential rate for subsidence reversal through permanent flooding of the land surface. This larger-scale experimental study has been monitored for land surface elevation, vegetation dynamics, water quality, and carbon flux dynamics in comparison with neighboring agricultural production [Miller, 2011; Miller *et al.*, 2008]. Our research questions focus on the magnitude and direction of atmospheric carbon fluxes through concurrent measurements of plant photosynthesis, ecosystem respiration, and CH<sub>4</sub> production and emission over seasonal to annual time scales. We sought to compare these fluxes from early (2002–2003) and later successional stages (2010–2011) of marsh development and considered changes over this period by coordinating with additional metrics tracked during study. Through our monitoring efforts, we show that (1) daily net CO<sub>2</sub> uptake was considerably smaller in the later stages of wetland development most likely due to reduced wetland plant photosynthesis, and (2) CH<sub>4</sub> emissions were large in 2010–2011, and likely similar in 2002–2003. The data illustrate the importance of CH<sub>4</sub> emissions and their potential in the annual GWP balance of a restored peat-building marsh. Despite years of relatively high productivity, variability in the exchange of atmospheric CO<sub>2</sub> and CH<sub>4</sub> observed in this study illustrates that extrapolating long-term carbon dynamics from short-term observations may be inaccurate, thus requiring management techniques that maintain consistent carbon storage rates and/or more comprehensive monitoring and modeling approaches [Bonn *et al.*, 2014].

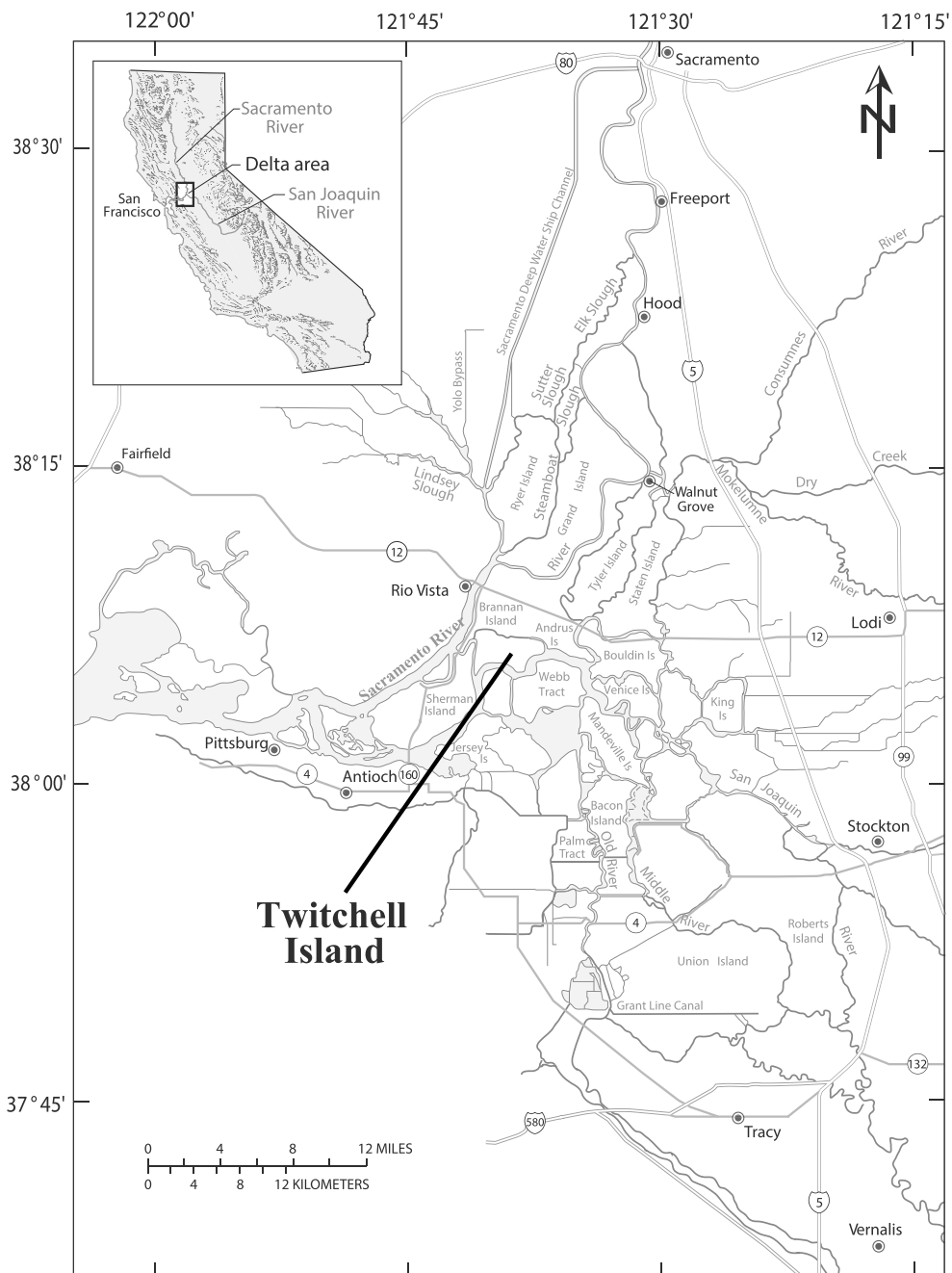


**Figure 1.** The restored, impounded wetland is located on Twitchell Island in the central Sacramento-San Joaquin Delta.

## 2. Methods

### 2.1. Site Description

Our study site was a restored, impounded freshwater wetland on Twitchell Island ( $38.1068^{\circ}\text{N}$ ,  $121.6465^{\circ}\text{W}$ ), located in the central Sacramento-San Joaquin Delta, California, USA (hereafter, the Delta; Figure 1). Historically, the Delta was a tidal fresh water marsh system in dynamic equilibrium with sediment transport, tectonic processes, and sea level rise [Mount and Twiss, 2005]. Sediment cores indicate that rich organic (peat) soils up to 15 m thick formed over the past 6700 years, consisting of organic plant fragments of bulrushes (*Schoenoplectus* spp.), cattails (*Typha* spp.), and reeds (*Phragmites* spp.), and inorganic components of alluvial silt and clay [Drexler et al., 2009a, 2009b]. Peat soils on Twitchell Island are classified in the Rindge Series as

euic, thermic Typic Medisaprists, formed from tule and reed plant residuals as well as mixed alluvial silts and clays from surrounding Sierra Nevada and Coastal Mountain ranges [Bossio *et al.*, 2006; Drexler *et al.*, 2009a, 2009b]. Fleck *et al.* [2007] estimates that approximately 4.5 m of peat soil remains under the wetland; however, the upper 1.5 m of soil underwent repeated agricultural draining cycles, altering the structure and reactive properties from preagricultural development. Prior to the construction of the wetland, the site was in agricultural production since the midnineteenth century [Miller *et al.*, 2008], typically *Zea mays* L. [Fleck *et al.*, 2004].

The wetland was constructed in 1997 to test the extent to which wetlands could slow oxidation of the underlying peat soils and if wetland plants could be used to accrete land surface in subsided Delta islands. Soil was excavated and used to build a perimeter berm around a basin that was leveled to approximately 4.5 m below sea level [Miller and Fujii, 2010]. Water levels were maintained at 55 cm using weirs, similar to hydrological management of rice fields, with water fed by siphon from the San Joaquin River (Figure S1 in the supporting information). Other studies at the site report estimated mean flow rates to be  $900 \pm 200$  L/min and approximate residence time of 13 days [Gamble *et al.*, 2003; Miller *et al.*, 2008]. They also report that specific conductance varied by season and ranged from 0.1 to 1.1  $\mu\text{S}/\text{cm}$ , while periodic samples of pH ranged from 7 to 8.5, with a mean value of 7.5, and dissolved oxygen was above 50% measured at the inlet [Miller *et al.*, 2008]. In 2010, the flow rate was reduced to 400 L/min—sufficient to minimize outflow and maintain the water level at 55 cm from the peat surface. A more detailed description of the study site and history can be found in Miller *et al.* [2008] and Miller and Fujii [2010].

To establish the wetland, initial populations of hardstem bulrush (*Schoenoplectus acutus*) were planted immediately following construction. By the summer of 1999, the plant community composition developed into a mosaic of roughly half open water and submerged aquatic vegetation, and half-emergent vegetation that included the planted bulrush and large areas of volunteer cattails (*Typha* spp.) [Miller and Fujii, 2010]. Vegetation mapping and field surveys from 2003 to 2012 indicate no major shifts in vegetation coverage, with the same observed distributions of open water versus emergent species since 2003 [Byrd *et al.*, 2014]. Over a 10 year period (1997–2008), the emergent wetlands accreted on average 28–47 cm [Miller *et al.*, 2008] of belowground detrital biomass. Miller and Fujii [2010] reported that mean annual emergent marsh carbon inputs into the wetland, as net primary productivity (NPP), ranged from 1295 to 2806  $\text{g C m}^{-2}$  with the highest and lowest NPP recorded in 1999 and 2000, respectively. They reported NPP values of  $2581 \text{ g C m}^{-2}$  in 2001 and  $1358 \text{ g C m}^{-2}$  in 2006. NPP apparently continued to decline slowly to as recently as 2012 [Byrd *et al.*, 2014]. Further, the area extent of emergent marsh had only a modest increase since 1999 [Miller and Fujii, 2010], and the absorption or reflection of incoming photosynthetically active radiation measured by Schile *et al.* [2013] suggests the presence of dense plant litter layer. The amount of dead material present as thatch in the wetland appears to have increased over this period, supported by changes in satellite data (normal difference vegetation index, NDVI) during August from 2002 to 2012 (see supporting information for further details).

## 2.2. Regional Climate

Regional climate in the Delta is classified as Mediterranean, characterized by warm, dry summers and cool, wet winters. The mean annual values of air temperature, solar radiation, and precipitation were  $15.11 \pm 0.58^\circ\text{C}$ ,  $6566 \pm 362 \text{ MJ m}^{-2}$ , and  $325 \pm 120 \text{ mm}$ , respectively. These values were from the nearby climate station on Twitchell Island (California Irrigation Management Information System (CIMIS) station #140), approximately 1 km to the NW of the study site and represents the period between 1997 and 2015. Outside the winter months, Twitchell Island experiences a persistent wind from the west, usually peaking in the late afternoon and evening, but elevated wind speeds occur throughout the diurnal period (Figure S2). Most flux studies experience higher percentages of missing data due to stable conditions that form at night and early morning hours [Aubinet *et al.*, 2012; Moffat *et al.*, 2007]; however, in our case, mean hour frictional velocity ( $u_*$ ;  $\text{m s}^{-1}$ ), a proxy for turbulence, remained high for both day ( $u_* = 0.5$ ) and night ( $u_* = 0.4$ ) conditions.

## 2.3. Greenhouse Gas and Micrometeorological Measurements

We used the eddy covariance (EC) technique, a statistical approach to measure the turbulent exchange of energy and mass between the atmosphere and land surfaces [Balocchi, 2003], to assess surface energy and  $\text{CO}_2$  fluxes during two separate periods: 2002–2003 and 2010–2011. Additionally, measurements of  $\text{CH}_4$  fluxes were collected from April of 2010 to April of 2011. Due to power disruptions, moisture, and

**Table 1.** Eddy Covariance and Ancillary Equipment<sup>a</sup>

	2002	2003	2010	2011
EC instrumentation height (m)	2.9	2.9	2.9	2.9
Data collection	Campbell Scientific CR23X & CR10X	Campbell Scientific CR23X & CR10X	Campbell Scientific CR1000/CFM & CR23X-AM16/32	Campbell Scientific CR1000/CFM & CR23X-AM16/32
Data measurement frequency and Storage	10 Hz, 30 min	10 Hz, 30 min	10 Hz, 10 Hz	10 Hz, 10 Hz
Sonic anemometer	Campbell Scientific CSAT3	Campbell Scientific CSAT3	Campbell Scientific CSAT3	Gill WindMaster
CO <sub>2</sub> /H <sub>2</sub> O analyzer	LI-COR LI7500	LI-COR LI7500	LI-COR LI7500	LI-COR LI7500
CH <sub>4</sub> analyzer	-	-	LGR FGGA	-
Air temperature/vapor pressure	Vaisala HMP45C	Vaisala HMP45C	Vaisala HMP45C	Vaisala HMP45C
Radiation	REBS Q7.1 net radiometer	REBS Q7.1 net radiometer	Kipp & Zonen CNR1	Kipp & Zonen CNR1
Water temperature	Campbell Scientific CS107B	Campbell Scientific CS107B	HOBO TMCx-HD Thermistor	HOBO TMCx-HD Thermistor
Ground heat flux	REBS HFP	REBS HFP	-	-

<sup>a</sup>A detailed description of instrumentation, data collection and processing, references and calibration frequency is presented in the supporting material.

changes in weather patterns, the majority of usable CH<sub>4</sub> flux data coincided with the peak growing season, between spring (April/May) and fall (October/November). In April of 2011, the bulk of the EC tower equipment was removed from the site; however, in late July, flux measurements of CO<sub>2</sub> and water vapor resumed. The tower location and instrument heights (2.9 m above the water surface) remained the same throughout the entire study.

Briefly, instrument and tower configuration were designed to capture the largest footprint possible within the wetland, while reducing the amount of data falling outside its rectangular configuration. Output from EC instrumentation, i.e. the sonic anemometer and gas analyzers were, recorded at 10 Hz and fluxes were either calculated and stored in the data logger or the raw data stored for further processing. Postprocessing included data despiking, maximum lag correlation, and wind coordinate rotation that aligns the local mean wind vector and removes the vertical and lateral means, sonic temperature correction, air density fluctuations, stationarity, and  $u^*$  and wind direction filtering. A detailed description of instrumentation, data collection and processing, references, and calibration frequency is presented in the supporting information. Auxiliary measurements of radiation, air and water temperature, and atmospheric humidity were collected at a frequency of 1 Hz, and half-hour averages were saved on a separate data logger. Table 1 summarizes instrumentation, measurement duration, and frequency for operational periods.

#### 2.4. Operational Periods

Data were analyzed and presented in the following manner: (1) all the available data for each year of the study, (2) peak growing season (August) when the system ran continuously during all four years, and (3) two gap-filled annual budgets from 15 April 2002 to 14 April 2003 and 15 April 2010 to 14 April 2011. Over the four years, approximately 20,000 half-hour means were calculated for each of the turbulent fluxes of sensible heat, latent heat, and CO<sub>2</sub>. For each year, the percentages of rejected or short missing data gaps for the three fluxes ranged from 38 to 60% (Table 2). These percentages are comparable to the typical range reported by *Moffat et al.* [2007] for missing data using the EC technique but differ from other studies, as the rectangular configuration of the wetland was responsible for almost 80% of the flux data removed via the wind direction filter and not low turbulent, nighttime conditions. For CH<sub>4</sub>, rejected or missing values were much higher, ranging from 66 to 88% in 2010 and 2011, respectively (Table 2), which were a result of ancillary power outages used to supply AC power to the CH<sub>4</sub> analyzer and in 2011, larger missing gaps of flux data in January and April when the analyzer was not running. Due to the extended breaks in measurements from year to year and higher percentages of rejected values outside the summer growing season, we examined the surface energy and CO<sub>2</sub> fluxes during the month of August as representation of peak growing season conditions [*Byrd et al.*, 2014]. Percentages of observed rejected or missing values were much lower, ranging from 17.4 to 27.1% (Table 2). To estimate the annual budgets between study periods, we chose 15 April through 14 April for both 2002–2003 and 2010–2011 as these dates represented the highest overlap of flux measurements between the two periods. For both years, the percentages of rejected or missing surface

**Table 2.** Periods of Flux Measurements and Quality Control Statistics

	2002	2003	2010	2011
Dates of operation	5/23–11/18	2/12–2/28, 4/11–11/21	4/23–11/23	1/30–3/28, 7/7–11/28
H rejected/missing (%)	38.0 <sup>a</sup> , 17.4 <sup>b</sup> , 67.2 <sup>c</sup>	43.0 <sup>a</sup> , 19.2 <sup>b</sup>	40.1 <sup>a</sup> , 23.5 <sup>b</sup> , 61.9 <sup>c</sup>	56.2 <sup>a</sup> , 20.1 <sup>b</sup>
LE rejected/missing (%)	38.0 <sup>a</sup> , 17.5 <sup>b</sup> , 67.3 <sup>c</sup>	43.3 <sup>a</sup> , 20.8 <sup>b</sup>	41.2 <sup>a</sup> , 24.1 <sup>b</sup> , 62.7 <sup>c</sup>	57.0 <sup>a</sup> , 21.4 <sup>b</sup>
CO <sub>2</sub> rejected/missing (%)	38.1 <sup>a</sup> , 17.6 <sup>b</sup> , 67.3 <sup>c</sup>	43.5 <sup>a</sup> , 21.0 <sup>b</sup>	44.6 <sup>a</sup> , 27.1 <sup>b</sup> , 65.0 <sup>c</sup>	60.0 <sup>a</sup> , 23.8 <sup>b</sup>
CH <sub>4</sub> rejected/missing (%)	-	-	65.7 <sup>a</sup> , 42.8 <sup>b</sup> , 77.9 <sup>c,d</sup>	87.5 <sup>d</sup>
Energy balance closure	0.76 <sup>a</sup> , 0.70 <sup>b</sup> , 0.76 <sup>c</sup>	0.91 <sup>a</sup> , 0.97 <sup>b</sup>	0.88 <sup>a</sup> , 0.74 <sup>b</sup> , 0.89 <sup>c</sup>	0.79 <sup>a</sup> , 0.85 <sup>b</sup>

<sup>a</sup>All available data by dates of operation for each year.<sup>b</sup>Growing season (August).<sup>c</sup>15 April through the following 14 April.<sup>d</sup>CH<sub>4</sub> analyzer not in operation from 23 November 2010 to 30 January 2011.

energy and CO<sub>2</sub> fluxes were 67% in 2002–2003 and 62–65% in 2010–2011, and 77.9% for CH<sub>4</sub> flux in 2010–2011 (Table 2). The higher percentages were mostly due to intermittent days or extended periods of missing data, from 19 November 2002 to 12 February 2003 and 23 November 2010 to 30 January 2011.

## 2.5. Energy Balance Closure

Energy balance closure was analyzed based on the three previously discussed data periods. We calculated the closure using an equal-weight energy balance ratio approach, similar to equation (2) in *Wilson et al.* [2002] or the “bulk method” described in *Franssen et al.* [2010]. We deviate from the methodology by summing the combined terms over the diel average, applying an equal weight to all times of the day. Using this approach, energy balance closure ranged from 0.76 to 0.91 for all available data in each year, from 0.70 to 0.97 for the month of August, and 0.76 and 0.89 for 2002–2003 and 2010–2011, respectively (Table 2). These values are typical and fall within the range of other terrestrial systems [*Stoy et al.*, 2013].

## 2.6. Gap Filling and Uncertainty Estimation

We used an artificial neural network (ANN) technique both to gap-fill missing fluxes and to estimate annual gap filled and random error uncertainty [*Moffat et al.*, 2007; *Richardson et al.*, 2008]. Rejected or missing half-hourly flux data were gap filled using ANN model inputs based on season, time of day, net radiation, water temperature, air temperature, and vapor pressure deficit [*Moffat et al.*, 2007]. There were very few instances where ancillary micrometeorological data were missing, although when this occurred, measurements of air temperature, vapor pressure, and radiation were supplemented from the nearby CIMIS climate station.

We followed the ANN optimization procedure outlined in *Knox et al.* [2015]. Briefly, we minimized bias in ANN training toward periods of greater data coverage (i.e., summer and daytime conditions), by representatively sampling natural clusters of the environmental data using the *k*-means algorithm in Matlab (MathWorks, Natick, MA, USA). The ANN was trained, validated, and tested each using one third of the representatively sampled data [*Papale and Valentini*, 2003]. Starting weights for the ANN nodes were reinitialized 10 times to avoid local minima. To facilitate generalizability, four different ANN architectures of increasing complexity were tested, and the simplest architecture was chosen for which increasing complexity resulted in less than a 5% gain in model accuracy. This entire procedure was repeated with 20 resampled sets of the data used to train, test, and validate the ANN. Missing half-hour fluxes were replaced by the median value from the 20 resultant predictions.

The annual cumulative uncertainty from gap-filled data and random measurement error was estimated as the variance of 20 ANN-modeled time series. For gap-filled values, the variance of the ANN-modeled output includes both gap filled and random uncertainty, as the residuals of the highly tuned ANN model provide a good, if not conservative estimate of the random flux uncertainty [*Moffat et al.*, 2007; *Richardson et al.*, 2008]. The random errors in EC fluxes follow a double exponential distribution with a standard deviation that varies with flux magnitude [*Richardson and Hollinger*, 2005]. Here we computed the random uncertainty of measured values by using the residuals of the median ANN predictions to parameterize the double exponential distribution according to flux magnitude [*Moffat et al.*, 2007], binned every 5  $\mu\text{mol m}^{-2} \text{s}^{-1}$  for CO<sub>2</sub> flux and 50  $\eta\text{mol m}^{-2} \text{s}^{-1}$  for CH<sub>4</sub>. For each measured value in the time series, we drew 100 random errors using the appropriately parameterized binned distribution, estimating the random flux uncertainty from the variance.

The annual cumulative uncertainty was computed following *Richardson and Hollinger* [2007] by adding the cumulative gap filling and random measurement uncertainties in quadrature.

We minimized uncertainty due to systematic measurement bias through a careful study design, instrument siting, frequent calibration, and proper processing procedures [Aubinet *et al.*, 2012]. The effects of three potential systematic biases—high-frequency loss (low-pass filtering), low-frequency loss (high-pass filtering), and the differences in heating of the open-path EC equipment compared to ambient air [Burba *et al.*, 2008]—were tested on a subset of summer, growing season data. Results from a one-way analysis of variance (ANOVA) in MATLAB (MathWorks, Natick, MA, USA) indicated there were no significant differences ( $p=0.1673$ ) between data not corrected and data corrected for the three systematic biases or any combination of the three. We acknowledge these potential biases, where correcting for high-frequency loss slightly increased CO<sub>2</sub> uptake during the day and respired CO<sub>2</sub> at night and where correcting for instrument heating slightly decreased CO<sub>2</sub> uptake during the day, we chose not to apply them here. The correction magnitudes were well within the random uncertainty of half-hourly CO<sub>2</sub> and energy flux measurements and an order of magnitude smaller than the Webb-Pearman-Leuning density corrections [Burba *et al.*, 2008; Webb *et al.*, 1980]. However, a known systematic bias in the closed-path measurements used for CH<sub>4</sub> was corrected prior to the ANN uncertainty estimation [Dettlo *et al.*, 2011]. High-frequency losses in closed-path analyzers such as that used in this study for CH<sub>4</sub> can be quite large [Aubinet *et al.*, 2012]. To correct this bias, we followed the approach of Dettlo *et al.* [2011] by developing a wind speed-dependent correction factor for the closed-path measurements using the ratio of CO<sub>2</sub> measured by the closed-path analyzer to that measured using an open-path analyzer (LI7500). A linear fit was calculated between this ratio and the wind speed for conditions that were dominated by photosynthetic activity or when the CO<sub>2</sub> flux was less than  $-5 \mu\text{mol CO}_2 \text{ m}^{-2} \text{ s}^{-1}$  [Dettlo *et al.*, 2011]. As with Dettlo *et al.* [2011], at low wind speeds the correction factor was negligible, but an increase in wind speed increased the correction. Uncertainty due to this correction was incorporated into the overall ANN-based assessment of measurement uncertainty by adjusting each half-hour average in the time series to include a randomly assigned error such that the assigned errors together represent the probability distribution of error within the 95% confidence interval of the correlation between the measurement ratio and wind speed.

## 2.7. NEE Partitioning

NEE of CO<sub>2</sub>, measured directly by the EC technique, is the net balance between gross ecosystem production (GEP) and ecosystem respiration (ER):

$$\text{NEE} = \text{GEP} + \text{ER} \quad (1)$$

where negative GEP values represent a net flux of carbon input from the atmosphere to the wetland and positive ER values represent the carbon output from the wetland to the atmosphere. We assume that GEP is zero at night, in the absence of photosynthesis. NEE is the integrated value of GEP and ER, where negative NEE is the net uptake of CO<sub>2</sub> into the wetland and a positive NEE indicates a net CO<sub>2</sub> loss from the combined effects of autotrophic and heterotrophic respiration under reduced or the absence of photosynthesis. In order to estimate GEP and ER, we follow the flux-partitioning algorithm described in Reichstein *et al.* [2005] that uses temperature estimated nighttime respiration values and then extrapolate the results to estimate daytime values of ER using light response curves. As others have found [e.g., Desai *et al.*, 2008], this modeled approach may be sensitive to which temperature parameter is used, i.e., water temperature ( $T_w$ ), air temperature ( $T_a$ ), or vegetation surface temperature ( $T_{sfc}$ ), when available. Here we present GEP and ER values using  $T_a$  modeled ER values as  $T_a$  had the longest, continuous data set and testing showed that there was very little difference in the modeled values between all three temperatures.

## 2.8. Statistics

Statistical analysis was performed using a one-way analysis of variance (ANOVA) in MATLAB (MathWorks, Natick, MA, USA). Tukey's honestly significant difference criterion with a  $p < 0.001$  was used to identify significant differences between (1) the annual variation in environmental variables: solar radiation ( $R_s$ ), net radiation ( $R_n$ ), air temperature ( $T_a$ ), water temperature ( $T_w$ ), vapor pressure deficit (VPD), wind speed (WS), and precipitation (PPT), (2) average daily flux values of NEE, GEP, and ER with environmental variables of  $R_n$ ,  $T_a$ ,  $T_w$ , VPD, and WS, and (3) to compare the fluxes of NEE, GEP, and ER between study periods.

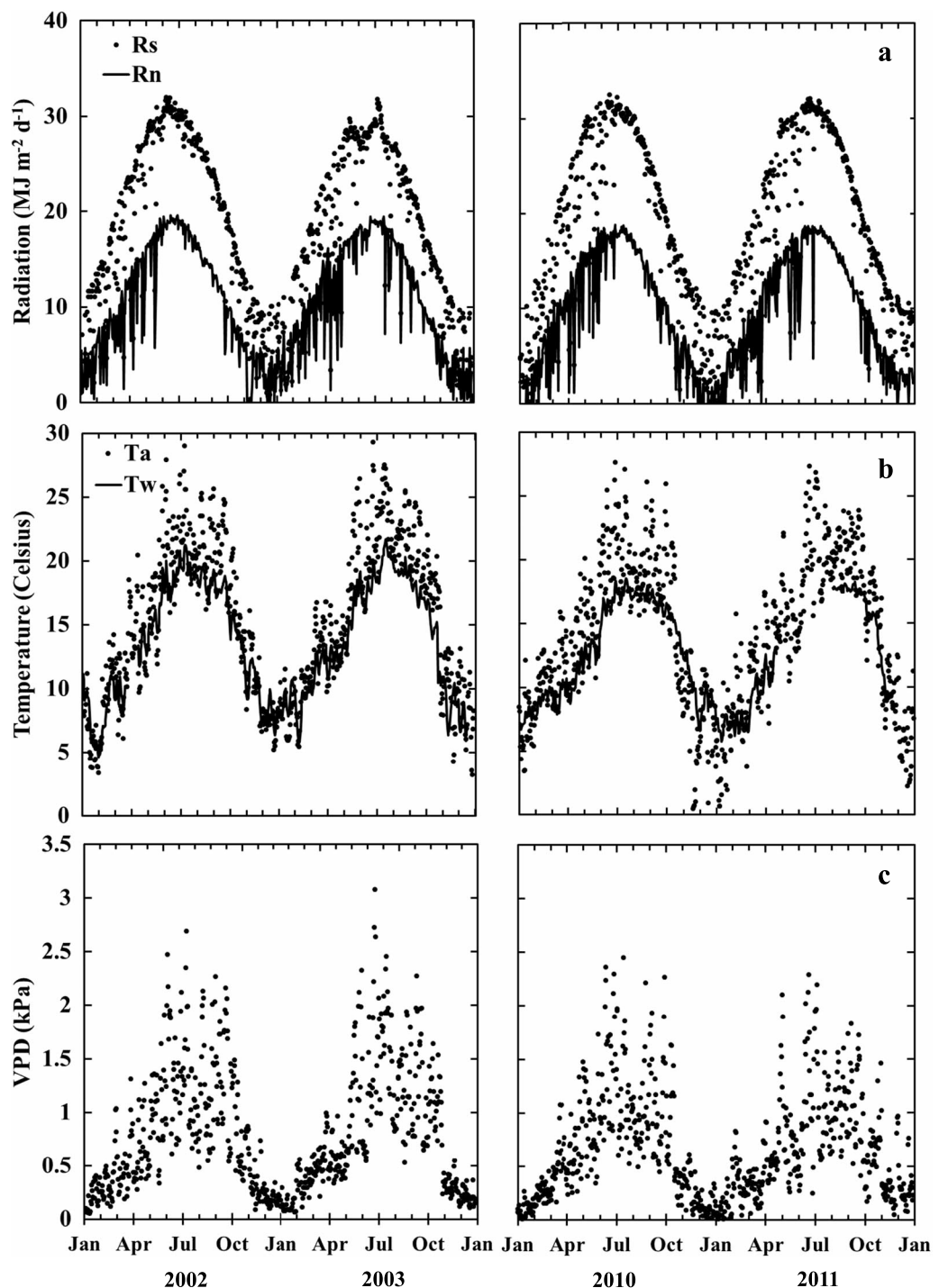


**Figure 2.** Daily-integrated values of (a) shortwave ( $R_s$ ) and net radiation ( $R_n$ ), (b) air ( $T_a$ ) and water temperatures ( $T_w$ ), and (c) vapor pressure deficit (VPD). Patterns in the annual plots of environmental conditions show typical Mediterranean climate conditions in the Sacramento-San Joaquin Delta region with maximum values of radiation, temperature, and VPD in the summer and minimum values in the winter. Patterns and magnitude of these conditions were similar for all four years, except for air and water temperatures in 2010 and 2011 when winter air temperatures and summer water temperatures were a few degrees lower.

**Table 3.** Average Annual and Daily-Integrated Environmental Conditions From 2002–2003 to 2010–2011: Solar Radiation ( $R_s$ ), Net Radiation ( $R_n$ ), Air Temperature ( $T_a$ ), Water Temperature ( $T_w$ ), Vapor Pressure Deficit (VPD), Wind Speed (WS), and Precipitation (PPT)<sup>a</sup>

Year	$R_s$ (MJ m <sup>-2</sup> yr <sup>-1</sup> )	$R_n$ (MJ m <sup>-2</sup> yr <sup>-1</sup> )	Average Daily $T_a$ (Min, Max) (°C)	Average Daily $T_w$ (Min, Max) (°C)	Average Daily VPD (Min, Max) (kPa)	Average Daily WS (Min, Max) (m s <sup>-1</sup> )	PPT January–December (mm)
2002	6839 <sub>A</sub>	3809 <sub>A,B,C</sub>	14.8 <sub>A,B</sub> (3.4, 29.0)	13.5 <sub>A</sub> (4.6, 21.3)	0.8 <sub>A,B</sub> (0.05, 2.7)	2.1 <sub>A</sub> (0.6, 6.6)	309 <sub>A</sub>
2003	6374 <sub>A</sub>	3839 <sub>B</sub>	15.5 <sub>A</sub> (3.2, 29.3)	13.8 <sub>A</sub> (5.8, 21.7)	0.8 <sub>A</sub> (0.06, 3.1)	2.1 <sub>A</sub> (0.5, 6.0)	295 <sub>A</sub>
2010	6581 <sub>A</sub>	3326 <sub>C</sub>	14.0 <sub>B</sub> (-2.4, 27.7)	12.6 <sub>B</sub> (6.6, 18.5)	0.7 <sub>B</sub> (0.0, 2.4)	3.2 <sub>B</sub> (0.9, 8.4)	468 <sub>A</sub>
2011	6693 <sub>A</sub>	3530 <sub>A,B,C</sub>	14.1 <sub>B</sub> (-0.7, 27.4)	12.1 <sub>B</sub> (5.7, 18.2)	0.7 <sub>B</sub> (0.0, 2.3)	3.1 <sub>B</sub> (0.8, 8.4)	344 <sub>A</sub>

<sup>a</sup>Capital letters indicate significant differences between the mean values (Tukey's honestly significant difference,  $p < 0.01$ ).

### 3. Results

#### 3.1. Annual Environmental Conditions

Environmental conditions over the two periods were evaluated and compared for significant differences (Figure 2 and Table 3). Daily averages of  $R_s$  and  $R_n$  were typical for the Mediterranean climate of the Delta region with minimum values less than 10 MJ m<sup>-2</sup> d<sup>-1</sup> during the winter for both variables and maximum values greater than 30 MJ m<sup>-2</sup> d<sup>-1</sup> for  $R_s$  and just under 20 MJ m<sup>-2</sup> d<sup>-1</sup> for  $R_n$  in the summer. We found that for all four years, mean annual  $R_s$  values were similar; however, the pattern of daily values of  $R_n$  throughout the year was significantly different and enough to create differences in the annual means. Seasonal patterns of VPD and air temperatures were similar between years. Daily averages of VPD and  $T_a$  peaked during the summer at approximately 2.5 kPa and between 25 and 30°C, respectively. Within each study period, 2002–2003 and 2010–2011, we found VPD and  $T_a$  to be similar. We also found that these variables were similar between 2002, 2010, and 2011. Average daily wind speeds were found to be similar within, but different between study periods, ranging from 0.5 to 8.4 m s<sup>-1</sup> and were predominantly from the west in the summer, but were more variable outside the summer growing season (Figure S2).

Annual differences in environmental conditions for all four years, ranged from as low as 7% ( $R_s$ ) to as high as 49% (PPT) (Table 3). When averaged, total annual  $R_n$  values were higher in 2002 and 2003 (3824 MJ m<sup>-2</sup> yr<sup>-1</sup>) compared to 2010 and 2011 (3428 MJ m<sup>-2</sup> yr<sup>-1</sup>). Average annual  $T_a$  across all four years was 14.6°C, 0.5°C lower than both the CIMIS long-term average (1997–2015) and Antioch climate station (1949–1999) [Hatala et al., 2012]. The difference in average  $T_a$  was 1.5°C for all four years, which was slightly higher than the annual variability of 1.3°C reported for a temperate wetland in Southern California but lower than the interannual variability for other terrestrial systems compiled in Rocha and Goulden [2008]. Average  $T_w$  was found to be significantly different and lower in 2010 and 2011; however, minimum temperatures in 2010 were 2°C warmer compared to 2002 (Table 3). Average annual wind speeds were also found to be significantly different between years and greater in 2010 and 2011 (~1 m s<sup>-1</sup>), while maximum daily average wind speeds were close to 2 m s<sup>-1</sup> higher compared to 2002 and 2003. It is important to note that the maximum wind speeds occurred during the winter and were caused by the passage of low-pressure systems. Sustained summer, afternoon winds were similar if not slightly higher in the first study period.

We also tested for significant differences in environmental conditions during the spring and summer (1 May to 30 September) for all four years to determine if there were conditions that may have influenced the wetland vegetation during the peak growing season (not shown here). Results from the test showed that the spring and summer means were similar to results of the annual mean testing (Table 3), except for  $R_n$  and  $T_w$ .  $R_n$  values were found to be similar in all four years as this period is characterized by clear and warm conditions.  $T_w$  was interesting in that 2011 became similar to 2002 and 2003, while 2010 was significantly different from the three other years.

#### 3.2. Variability in Energy Partitioning and Carbon Dioxide Uptake

For both study periods, daily-integrated surface energy and CO<sub>2</sub> fluxes followed the expected seasonal pattern, with maximum energy flux and CO<sub>2</sub> uptake during the peak growing season (Figure 3). Maximum

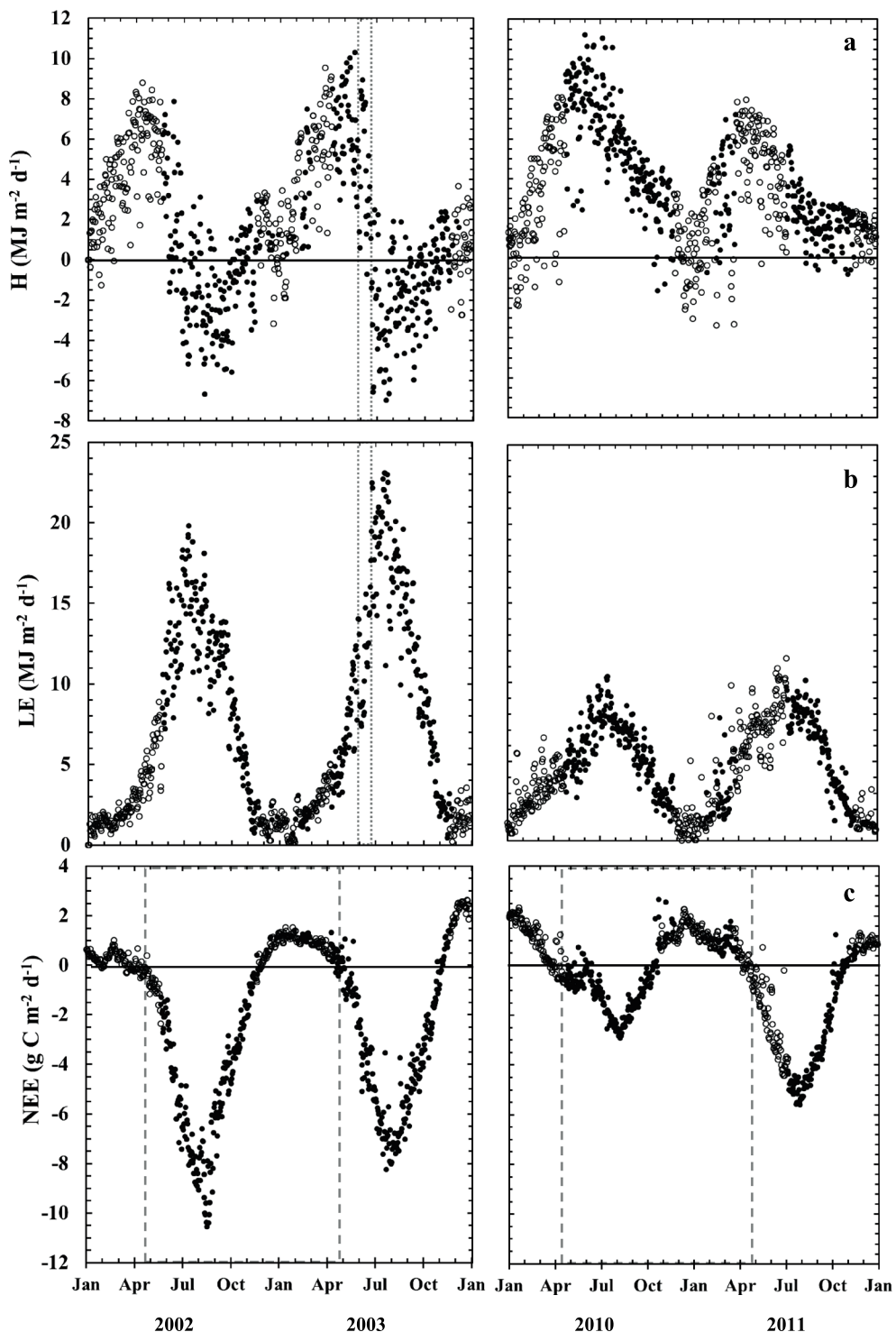


**Figure 3.** Daily averaged (a) sensible heat flux ( $H$ ), (b) latent heat flux ( $LE$ ), and (c) net ecosystem exchange (NEE) for years 2002–2003 and 2010–2011. Closed circles represent days when the eddy covariance system was in operation. Open circles represent days when the system was inoperable or there were no resolvable half-hour fluxes and daily values were estimated from the artificial neural network (ANN) gap-filling routine. The dotted area in the sensible and latent heat fluxes (2002 and 2003 plots) represents the period when there was a rapid transition of energy partitioning in the canopy (24 May through 27 June 2003). The dashed areas in the NEE plots represent the period used to calculate the annual cumulative sum.

positive values of sensible and latent heat fluxes and maximum negative values of NEE occurred during the spring and summer months, driven by high  $R_s$ , warm temperatures, and peak plant photosynthesis. Negative values of sensible heat, minimum values of latent heat, and positive values of NEE occurred during the fall and winter months as solar insolation decreased, temperatures cooled, and wetland plants became dormant.

Despite the similar seasonal timing between study periods, there were significant differences in both the overall magnitude and timing of surface energy and CO<sub>2</sub> fluxes, indicative of changes in wetland carbon sequestration potential. Most notably, sensible heat flux exhibited a large excursion from positive to negative values in 2002 and 2003, as more energy was made available for evaporation. No comparable pattern occurred in 2010 and 2011, and positive values were observed throughout late summer and fall (Figure 3a). The seasonality of the sensible heat flux was also different between study periods, though the seasonality of environmental conditions was consistent. For example, in 2003, the maximum sensible heat flux of 10 MJ m<sup>-2</sup> d<sup>-1</sup> was measured on 24 May and the minimum of -8 MJ m<sup>-2</sup> d<sup>-1</sup> was measured on 27 June. By comparison, in 2010, an equivalent maximum value of 11 MJ m<sup>-2</sup> d<sup>-1</sup> was reached on 7 July and a greater minimum value of -2 MJ m<sup>-2</sup> d<sup>-1</sup> occurred much later in the year (8 November) than the minimum observed in the earlier study period. Changes in both the timing and magnitude of the sensible heat flux suggest a change in how energy was partitioned between the two study periods. Negative fluxes of sensible heat in 2002–2003 indicate that sensible heat was extracted from the atmosphere, increasing rates of latent heat. Conversely, in 2010–2011, positive fluxes of sensible heat dissipated energy from the canopy to the atmosphere throughout the growing season.

The difference between study periods was also evident in the maximum values and seasonality of the measured latent heat flux (Figure 3b). In all four years of the study, maximum daily averages peaked during the growing season and were at a minimum during the winter, coinciding with changes in plant phenology and VPD. Peak summer values of latent heat flux in the early study period were above 20 MJ m<sup>-2</sup> d<sup>-1</sup> for both years, while they did not exceed 12 MJ m<sup>-2</sup> d<sup>-1</sup> in the later study period. The observed latent heat flux in 2003 quickly rose from 6.7 MJ m<sup>-2</sup> d<sup>-1</sup> on 24 May to a maximum of 23.6 MJ m<sup>-2</sup> d<sup>-1</sup> on 27 June, coinciding with the sharp decline in sensible heat flux, and then declining to a minimum (~1 MJ m<sup>-2</sup> d<sup>-1</sup>) in late November. By comparison, in 2010, the latent heat flux had a more dampened signal rising from approximately 5 MJ m<sup>-2</sup> d<sup>-1</sup> in May to 11 MJ m<sup>-2</sup> d<sup>-1</sup> on 7 July, and then declining to approximately 1 MJ m<sup>-2</sup> d<sup>-1</sup> in November. The sharp rise in latent heat flux and corresponding decline in sensible heat flux in 2003 indicate the earlier study period exhibited a greater modulation of energy fluxes due to photosynthetic activity, most likely due to higher green leaf area and canopy density. In 2010, both sensible and latent heat fluxes closely tracked the influx of solar radiation and were similar in magnitude throughout the year.

As expected, the seasonal pattern of NEE more closely tracked patterns in latent heat flux and the seasonal growth of the wetland canopy (Figure 3c). Greatest CO<sub>2</sub> uptake was observed in all years from late July through November; however, as with the surface energy fluxes, there were significant differences between study periods. Higher uptake rates were observed in 2002 and 2003 with mean daily NEE values reaching -10.6 g C m<sup>-2</sup> d<sup>-1</sup> and -8.8 g C m<sup>-2</sup> d<sup>-1</sup>, respectively. In 2010, CO<sub>2</sub> uptake was greatly reduced, with NEE values less than one third of those measured in the early study period (-2.9 g C m<sup>-2</sup> d<sup>-1</sup>). In 2011, maximum CO<sub>2</sub> uptake was -5.6 g C m<sup>-2</sup> d<sup>-1</sup>, nearly twice that observed in 2010; however, uptake was approximately one half to one third of the maxima observed in 2002 and 2003.

### 3.3. Gross Ecosystem Productivity and Respiration During the Peak Growing Season

We compared modeled gross ecosystem productivity (GEP) and respiration (ER) for the month of August to examine differences between the peak growing seasons of the two study periods (Figure 4). NEE values for all years indicated that the wetland was a carbon sink during the month of August. As observed with the longer time series, the average CO<sub>2</sub> uptake was approximately twice as large during August of the earlier study period (2002 and 2003) than in August of the later study period (2010 and 2011). August daily average ER was higher in the early study period than the late study period, but the difference in ER rates between study periods was far lower than for GEP. ER in the early study period averaged 5.0 g C m<sup>-2</sup> d<sup>-1</sup>, 39% higher than that seen in the later study period, which averaged 3.6 g C m<sup>-2</sup> d<sup>-1</sup>. The reduced ER rates in 2010 and 2011, may be a function of lower air and water temperatures that were measured in the later study period (~1°C; Table 3) [see Davidson *et al.*, 2006]. However, we cannot rule out that the reduction in 2010 and

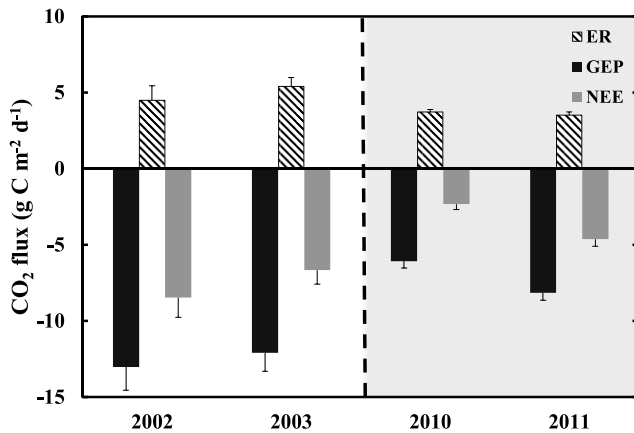


**Figure 4.** Average daily rates of gross ecosystem production (GEP), ecosystem respiration (ER), and net ecosystem exchange (NEE) for the month of August, a representation of peak growing season conditions. Average values of GEP, ER, and NEE ranged from  $-13.0 \text{ g C m}^{-2} \text{ d}^{-1}$  in 2002 to  $-6.1 \text{ g C m}^{-2} \text{ d}^{-1}$  in 2010,  $5.4 \text{ g C m}^{-2} \text{ d}^{-1}$  in 2003 to  $3.5 \text{ g C m}^{-2} \text{ d}^{-1}$  in 2011, and  $-8.5 \text{ g C m}^{-2} \text{ d}^{-1}$  in 2002 to  $-2.3 \text{ g C m}^{-2} \text{ d}^{-1}$  in 2010, respectively. Error bars represent the standard deviation from all the daily flux values during the month of August.

( $56.3 \pm 6.4 \text{ g C m}^{-2} \text{ yr}^{-1}$ ) in comparison to values reported in the literature [Petrosescu *et al.*, 2015]. As observed in other studies, the seasonal variation of CH<sub>4</sub> emissions was related to that of latent heat flux and NEE, seasonal growth of the wetland plant canopy, peak seasonal temperatures, and bulk or pressurized convective flow through emergent vegetation [Chanton *et al.*, 1993; Garnet *et al.*, 2005; Kim *et al.*, 1999]. Greatest emissions ( $188.6\text{--}375.9 \text{ mg C m}^{-2} \text{ d}^{-1}$ ) occurred between July and September, and minimum values ( $38.1\text{--}102.4 \text{ mg C m}^{-2} \text{ d}^{-1}$ ) occurred in late January through March (Figure 5). On a molecular carbon basis, the peak in CH<sub>4</sub> flux ( $375.9 \text{ mg C m}^{-2} \text{ d}^{-1}$ ) makes up a small percentage (13.0%) of peak season

2011 may also be attributed to lower autotrophic respiration, as GEP and aerenchyma pathway system were reduced [Aubrey and Teskey, 2009], and/or lower heterotrophic respiration due to reduced labile carbon availability [Davidson *et al.*, 2006; Gu *et al.*, 2004]. Nevertheless, we surmise that the difference in NEE between study periods was driven by differences in GEP rather than respiration, with GEP in the earlier study period averaging  $12.6 \text{ g C m}^{-2} \text{ d}^{-1}$  or 176% compared to the later study period, which averaged  $7.1 \text{ g C m}^{-2} \text{ d}^{-1}$ .

### 3.4. Seasonal CH<sub>4</sub> Fluxes

CH<sub>4</sub> emissions were measured in the later study period from 23 April 2010 to 28 March 2011 to quantify the annual ecosystem carbon balance and global warming potential (GWP). The measured annual CH<sub>4</sub> flux was high

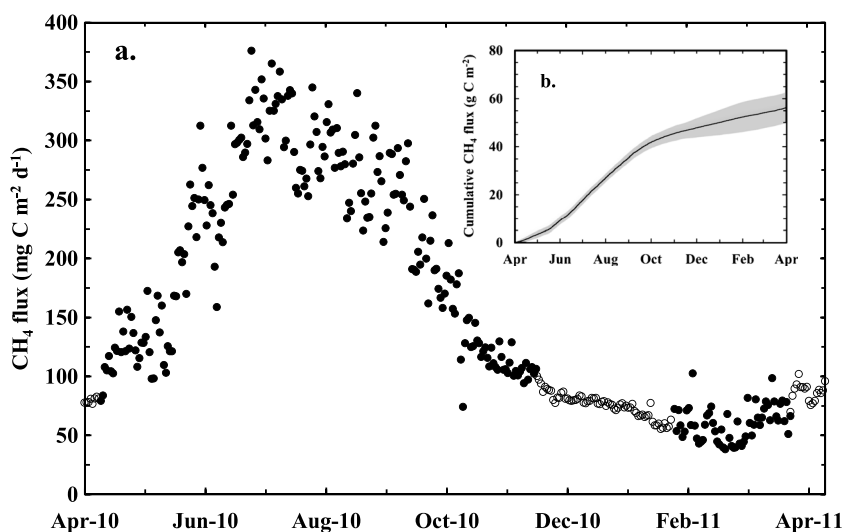


**Figure 5.** (a) Daily-integrated CH<sub>4</sub> fluxes from 15 April 2010 through 15 April 2011. Closed circles represent days when the eddy covariance system was in operation. Open circles represent days when the system was inoperable or there were no resolvable half-hour fluxes and daily values were estimated from the artificial neural network (ANN) gap-filling routine. CH<sub>4</sub> fluxes increased during the spring, peaked in late July and August, and declined to a minimum in January and February. Seasonal differences correspond to canopy growth, air temperature, and are inversely proportional to daily net ecosystem exchange (NEE) rates. (b) Cumulative daily CH<sub>4</sub> fluxes for the same period resulted in an annual CH<sub>4</sub> flux of  $56.3 \text{ g C m}^{-2}$ . Gray shaded area represents the uncertainty at the 95% confidence interval from the 20 predictions of the ANN gap-filling routine for both measured and ANN gap-filled values.

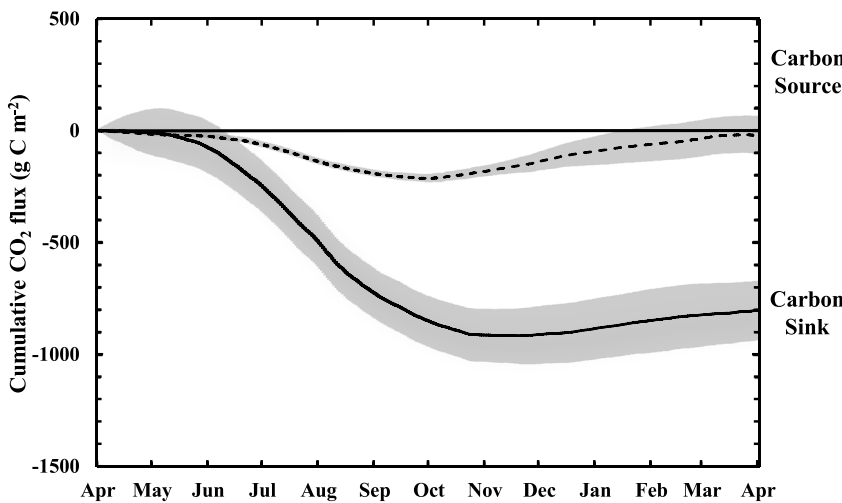


**Figure 6.** Cumulative net ecosystem exchange (NEE) plotted from 15 April 2002 through 15 April 2003 (solid line) and 15 April 2010 through 15 April 2011 (dashed line). Gray shaded area represents the uncertainty at the 95% confidence interval from the 20 predictions of the artificial neural network (ANN) gap-filling routine for both measured and ANN gap-filled values. In general, uptake of CO<sub>2</sub> was greater in 2002–2003 compared to 2010–2011, a possible indication that conditions were more favorable for potential wetland carbon sequestration and as a result, the wetland was a carbon sink. Conversely, less favorable conditions in 2010–2011 resulted in a near neutral carbon budget.

photosynthetic uptake in 2010 ( $-2.9 \text{ g C m}^{-2} \text{ d}^{-1}$ ). However, using these peak season numbers and the GWP for CH<sub>4</sub> as 34 times the CO<sub>2</sub> equivalent (100 year time horizon; Myhre *et al.* [2013]), the CO<sub>2</sub> equivalent from the CH<sub>4</sub> flux was 158.6% ( $4.6 \text{ g C m}^{-2} \text{ d}^{-1}$ ) of the CO<sub>2</sub> sequestered through photosynthesis (Figure 3;  $-2.9 \text{ g C m}^{-2} \text{ d}^{-1}$ ).

### 3.5. Cumulative Annual CO<sub>2</sub> and CH<sub>4</sub> Budgets

Comparing the cumulative annual NEE budgets from 15 April 2002 to 14 April 2003 and 15 April 2010 to 14 April 2011 revealed that while the wetland was a net CO<sub>2</sub> sink in 2002–2003 ( $-804.2 \pm 131.5 \text{ g C m}^{-2} \text{ yr}^{-1}$ ), it was near carbon neutral in 2010–2011 ( $-21.1 \pm 83.1 \text{ g C m}^{-2} \text{ yr}^{-1}$ ) (Figure 6). The biggest difference between the two periods was observed during the summer growing season, where in 2002–2003 NEE was almost 4 times greater than the rate measured in 2010–2011. In both periods, winter respiration reduced the cumulative annual NEE magnitude. CH<sub>4</sub> emissions remained positive throughout the year in 2010–2011 with the highest rates observed during the summer growing season (Figure 5a). The annual cumulative CH<sub>4</sub> flux in 2010–2011 (Figure 5b;  $56.3 \text{ g C m}^{-2} \text{ yr}^{-1} \pm 6.4 \text{ g C m}^{-2} \text{ yr}^{-1}$ ) was small on a molar basis in comparison to the cumulative annual CO<sub>2</sub> uptake in 2002–2003 (Figure 6;  $-804.2 \pm 131.5 \text{ g C m}^{-2} \text{ yr}^{-1}$ ) but of similar magnitude to the cumulative annual CO<sub>2</sub> uptake in 2010–2011 (Figure 6;  $-21.1 \pm 83.1 \text{ g C m}^{-2} \text{ yr}^{-1}$ ).

## 4. Discussion

### 4.1. Evaluating Differences in Wetland Carbon Uptake

The contrast in the cumulative annual NEE from 2002–2003 ( $-804.2 \pm 131.5 \text{ g C m}^{-2} \text{ yr}^{-1}$ ) to 2010–2011 ( $-21.1 \pm 83.1 \text{ g C m}^{-2} \text{ yr}^{-1}$ ) reveals that the magnitude of carbon uptake may be unpredictable, or that CO<sub>2</sub> uptake may be larger immediately following restoration, as suggested in Schrier-Uijl *et al.* [2014]. Based on the evidence from the seasonal timing and magnitude of sensible and latent heat fluxes, as well as the similarity in ER compared to GEP between study periods (Figure 4), the observed difference appears to reflect a change in wetland photosynthetic production. This is in agreement with biomass sampling, which demonstrated that plant production at the wetland progressively decreased from  $2581 \text{ g C m}^{-2} \text{ yr}^{-1}$  in 2001 to  $1358 \text{ g C m}^{-2} \text{ yr}^{-1}$  in 2006 [Miller and Fujii, 2010]. We note that the differences in magnitude and range in annual NEE measured in this study versus those reported by Miller and Fujii [2010] were likely due to the difference between the flux tower footprint and the more widely disbursed biomass sampling plots.

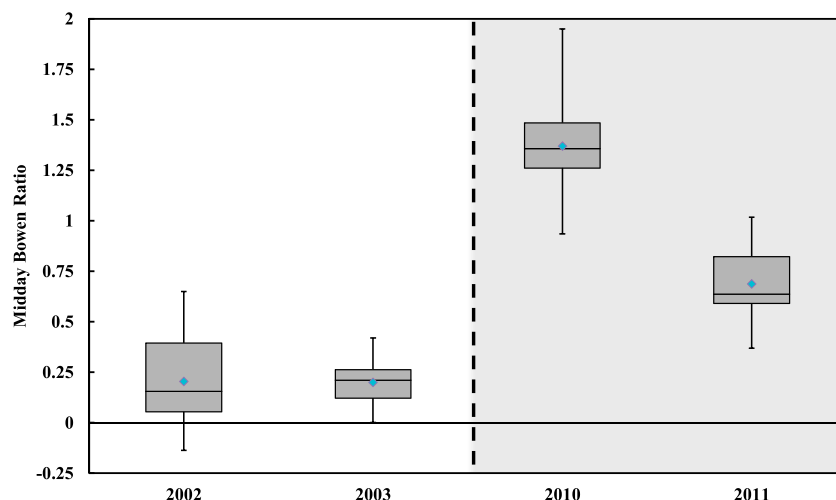


**Figure 7.** Average midday (1000–1400 local time) Bowen ratios (the ratio of sensible to latent heat fluxes) were compared for the month of August, representing peak growing season conditions. The diamond shape point represents the mean daily value for the month. The median or second quartile is represented by line in the box, while the top and bottom of the box represents the extent of the first and third quartiles, and the whiskers represent the maximum and minimum values. Average daily values were close to 0.2 in 2002 and 2003, 1.4 in 2010, and 0.7 in 2011. The interannual variability in midday Bowen ratios correspond to similar magnitude changes observed for fluxes of LE and CO<sub>2</sub> uptake, where the highest values were observed in 2002 and 2003, and lowest in 2010.

Differences in environmental factors do not explain the observed differences in photosynthetic activity between study periods. We compared mean daily values of GEP, ER, and NEE to environmental conditions ( $R_n$ ,  $T_a$ , VPD, WS and  $T_w$ ) for the peak growing season (August). Results revealed that GEP was most closely related to  $T_w$  ( $r^2$ : 0.54;  $p < 0.001$ ). However, we are aware of no direct mechanistic reason that the modest correlation in  $T_w$  can account for the observed threefold difference in sink strength between study periods. We surmise that shading can reduce  $T_w$ , a secondary effect rather than a driver, and conclude that  $T_w$  did not account for the observed differences between study periods. This agrees with the conclusion of *Rocha and Goulden* [2008] from a study of a freshwater marsh in Southern California, where they found no linkage between weather conditions and the interannual variability of NEE, ER, and GEP.

Strong evidence in this study suggests that the lower photosynthetic activity in the later study period is due to the buildup of senescent plant material of mostly dead *S. acutus* stems, as evidenced by the reduction in latent heat flux and CO<sub>2</sub> uptake. Senescent material can either absorb or reflect almost 100% of the incoming photosynthetically active radiation [Schile et al., 2013], preventing it from reaching the water surface and subsequent rhizome systems where young shoots growth is stimulated [Bonneville et al., 2008]. In the latter period of this study, it is likely that the presence of senescent material shaded water surfaces and impeded plant growth, consistent with our observations of reduced  $T_w$ , lower evaporation and transpiration rates, and resultant lower latent heat flux. This result is similar to *Goulden* et al. [2007], who found that the presence of a thick plant litter mat kept water temperatures lower, reduced rates of evaporation, and lowered overall evapotranspiration. That senescent plant material was more abundant in the later study period is indicated by automated photographic monitoring (Figures S3 and S4) and an evaluation of differences in August NDVI values between study periods (Landsat 7 ETM+; Figure S5). NDVI values within the tower footprint were higher during the earlier study period and declined from 2006 to 2010 (Figure S5), suggesting changes to the canopy structure may have altered interception of photosynthetically active radiation over time, consistent with the observed decline in latent heat flux and CO<sub>2</sub> uptake.

To assess the extent to which accumulated senescent plant material affected surface fluxes, we calculated the Bowen ratio, or the ratio of sensible heat versus latent heat, for all four years during the peak growing season. Average Bowen ratios, calculated from midday values (1000–1400 local time) for the month of August, were close to 0.2 in 2002 and 2003, 1.4 in 2010 and 0.7 in 2011 (Figure 7). The higher Bowen ratios observed in 2010 and 2011 indicate that more of the available energy dissipated as sensible heat. These results are similar to results presented by *Rocha and Goulden* [2008] where higher Bowen ratio values were observed in years

when NEE was lower, suggesting senescent material was a driver of the difference. It is instructive that the Bowen ratio values calculated for this study were lower than results presented in *Rocha and Goulden* [2008], where inundation at their site was seasonal rather than continuous, which would lower the effect of the senescent material on the energy balance. Values in this study are similar to values seen in the Florida Everglades [*Malone et al.*, 2014; *Schedlbauer et al.*, 2012], where inundation was more comparable.

#### 4.2. Implications

Given the interest in utilizing wetlands for carbon offset and trading programs [Galatowitsch, 2009], it is useful to examine both the difference in the annual atmospheric carbon mass balance and the concomitant influence of CH<sub>4</sub> on the GWP balance [Bridgman et al., 2006]. *Whiting and Chanton* [1993] estimated that on a molar basis, CH<sub>4</sub> emissions make up a small portion (roughly 3%) of the net daily CO<sub>2</sub> uptake from wetlands globally. However, when GWP is considered, the warming effect of CH<sub>4</sub> emitted from freshwater wetlands can strongly reduce or even exceed the cooling effect of photosynthetic CO<sub>2</sub> uptake [Brix et al., 2001; Herbst et al., 2011; Olson et al., 2013]. This study shows that CH<sub>4</sub> emissions can have a significant influence on both the carbon and GWP balances. The mass of carbon from annual CH<sub>4</sub> emissions measured in 2010–2011 was small (8%) on a molar basis ( $56.3 \pm 6.4 \text{ g C m}^{-2} \text{ yr}^{-1}$ ) compared to the CO<sub>2</sub> uptake in 2002–2003 ( $-804.2 \pm 131.5 \text{ g C m}^{-2} \text{ yr}^{-1}$ ). However, because CO<sub>2</sub> uptake in 2010–2011 was lower ( $-21.1 \pm 83.1 \text{ g C m}^{-2} \text{ yr}^{-1}$ ) than in 2002–2003, inclusion of CH<sub>4</sub> emissions in the overall carbon budget resulted in the wetland becoming a small net carbon source by mass ( $35.2 \pm 83.3 \text{ g C m}^{-2} \text{ yr}^{-1}$ ). Using a GWP for CH<sub>4</sub> that is 34 times that of CO<sub>2</sub> [Myhre et al., 2013], the GWP influence of CH<sub>4</sub> emissions in 2010–2011 was  $696.4 \pm 79.0 \text{ g C m}^{-2} \text{ yr}^{-1}$ , which far exceeded photosynthetic cooling in 2010–2011 and represents a value similar (opposite in sign) to the photosynthetic cooling of 2002–2003. We note that CH<sub>4</sub> emission at the Twitchell Island wetland represents one of the highest rates reported in the literature [Petrescu et al., 2015]. This finding adds further support to the growing evidence [e.g., Chu et al., 2014] that CH<sub>4</sub> plays a significant role in the carbon balance in freshwater wetlands, especially during periods of lower plant productivity.

To assess the extent to which the GWP balance of the wetland may have differed between study periods, we calculated the prospective annual carbon and GWP balances for 2002–2003 using the CH<sub>4</sub> emission values from 2010 to 2011, i.e., we assumed the CH<sub>4</sub> emission rate was similar for both periods. That this assumption is reasonable is supported by direct measurements previously published from static chamber flux measurements made at this wetland [Miller, 2011] showing CH<sub>4</sub> emissions to be relatively invariant, with median midday CH<sub>4</sub> emissions of  $13.8 \text{ mg C m}^{-2} \text{ h}^{-1}$  and an interquartile range from 8.2 to  $21.1 \text{ mg C m}^{-2} \text{ h}^{-1}$  between March and December 2000 through 2003. These chamber values are similar to midday fluxes measured in this study from April to December 2010, where the mean value was  $9.8 \text{ mg C m}^{-2} \text{ h}^{-1}$  and the range was from 2.4 to  $29.5 \text{ mg C m}^{-2} \text{ h}^{-1}$ . This supports that overall CH<sub>4</sub> emissions were presumably similar between the 2002–2003 and 2010–2011 study periods, and differences in emission ranges are most likely due to methodology and an increase in resolvable fluxes from the EC system.

Further supporting the notion that CH<sub>4</sub> emissions were similar between the two study periods are other studies showing that CH<sub>4</sub> fluxes can vary little over time, even in wetlands undergoing changes in succession or hydrological management. For example, a 6 year study at an unaltered postglacial northern latitude ombrotrophic bog by *Roulet et al.* [2007] showed annual CH<sub>4</sub> to be relatively small and consistent, with a mean of  $3.7 \pm 0.5 \text{ g C m}^{-2} \text{ yr}^{-1}$  ( $\pm 1$  standard deviation). During a four year study from 2005 to 2008, *Schrier-Uijl et al.* [2014] observed annual CH<sub>4</sub> fluxes to vary between  $13.2$  and  $15.4 \text{ g C m}^{-2} \text{ yr}^{-1}$ , 7 years after the conversion from an intensely agriculturally managed peatland to a grass/wetland polder. Even a newly restored wetland on an adjacent island in the Delta reported mean annual CH<sub>4</sub> fluxes of  $50 \pm 2 \text{ g C m}^{-2} \text{ yr}^{-1}$  from 2012 to 2014 despite large changes in CO<sub>2</sub> uptake [Sturtevant et al., 2016]. Moreover, *Chu et al.* [2014] only observed moderate variation in annual CH<sub>4</sub> fluxes from  $42.3$  to  $57.0 \text{ g C m}^{-2} \text{ yr}^{-1}$  in the case where hydrological management changed to a year-round inundation after decades of periodic lowering of summer water levels at a freshwater marsh on the shores of Lake Erie.

However, some studies report lower or variable CH<sub>4</sub> emission rates during earlier periods of wetland establishment. For instance, low CH<sub>4</sub> emission rates were observed the first year following conversion from corn and alfalfa production to rice cultivation at an adjacent site on Twitchell Island [Hatala et al., 2012]. Despite the high carbon peat soils found on Twitchell Island, they attributed the lower initial fluxes to the lack of labile

fresh plant material, but that in subsequent years the incorporation of rice straw was suggested to increase labile carbon and resultant CH<sub>4</sub> emissions [Knox *et al.*, 2015; Hatala *et al.*, 2012]. Lower CH<sub>4</sub> production was also observed after initial inundation of a degraded fen grassland in NE Germany [Hahn-Schoff *et al.*, 2011]. Here lower values were attributed to the competition between methanogens and iron- or sulfate-reducing bacteria and/or continued aerobic conditions in the upper peat soil layers. In this study, we do not believe the previous processes played a significant role as the wetland had been inundated for close to 5 years before EC flux measurements began in 2002 and the emergent macrophytic canopy was over 50% in coverage, providing sufficient labile carbon from fresh and dead plant material as well as root exudates.

Our study shows that in 2010–2011 the radiative forcing associated with the measured CH<sub>4</sub> emissions in combination with the reduced photosynthetic uptake of CO<sub>2</sub> was a large net GWP source to the atmosphere ( $675.3 \pm 114.7 \text{ g C m}^{-2} \text{ yr}^{-1}$ ). When we included 2010–2011 CH<sub>4</sub> emissions in the GWP balance for 2002–2003, GWP went from  $-804.2 \pm 131.5 \text{ g C m}^{-2} \text{ yr}^{-1}$  to near equilibrium at  $-107.8 \pm 153.4 \text{ g C m}^{-2} \text{ yr}^{-1}$ . Recomputing these results using a  $\pm 20\%$  uncertainty bound on the CH<sub>4</sub> emissions yields a GWP range from  $-247$  to  $34 \text{ g C m}^{-2} \text{ yr}^{-1}$ . This exercise shows that even over this broad range of potential variability, CH<sub>4</sub> can dramatically lower or even reverse the GWP balance.

Although simple GWP calculations are appropriate for evaluation of benefits in the context of carbon markets, Neubauer and Megonigal [2015] stress that continuous emission sources such as wetlands should be evaluated differently to account for the eventual new steady state in atmospheric concentrations. They introduce a new metric, the sustained flux GWP (SGWP), which varies over time to account for the changing radiative forcing balance in the atmosphere. Evaluating the wetland performance using this new metric reveals that wetland productivity and emissions in the more productive 2002–2003 period result in a SGWP of  $1161.2 \pm 259.3 \text{ g C m}^{-2} \text{ yr}^{-1}$  at 20 years,  $117.1 \pm 168.2 \text{ g C m}^{-2} \text{ yr}^{-1}$  at 100 years—the time scale relevant to carbon markets—and becomes a sink at 500 years ( $-517.6 \pm 135.6 \text{ g C m}^{-2} \text{ yr}^{-1}$ ). In contrast, using the wetland performance characteristics for the less productive study period, 2010–2011, yields a SGWP of  $1944.3 \pm 238.4 \text{ g C m}^{-2} \text{ yr}^{-1}$  at 20 years and  $900.2 \pm 133.7 \text{ g C m}^{-2} \text{ yr}^{-1}$  at 100 years, and still shows the wetland to be a significant SGWP source at 500 years ( $265.5 \pm 89.3 \text{ g C m}^{-2} \text{ yr}^{-1}$ ). Presuming that the 2010–2011 period represents future ongoing wetland performance, it appears that this wetland will be a SGWP source when integrated over time scales relevant to carbon offset and trading programs.

It is also important to realize that the EC study presented here did not account for carbon loss due to lateral and seepage flux of dissolved organic carbon (DOC) and dissolved inorganic carbon (DIC), which can be significant [Bergamaschi *et al.*, 2012]. We estimated the loss using data from Fleck *et al.* [2007], which examined DOC export from our study site, and based on these calculations, DOC export could account for approximately 12% of the measured cumulative annual NEE in 2002–2003 but a much greater fraction, approximately 36%, in 2010–2011. We could not find data that permitted us to estimate losses due to DIC seepage and export, so that term remains unconstrained but would further reduce the NEE. These results indicate that lateral and seepage fluxes of DOC can be important contributors to the net ecosystem carbon balance and need to be included in wetland monitoring where carbon accounting is a goal.

The trajectory of carbon sequestration potential for this wetland is not clear. It is possible that it will follow a trajectory, where the first few years are highly productive but at some point, the system reaches a steady state condition of reduced rates of CO<sub>2</sub> uptake. This idea is similar to what is described by Craft *et al.* [2003] in their conceptual model of salt marsh ecosystem development or suggested by Schrier-Uijl *et al.* [2014] that after restoration the ecosystem sink potential is higher before stabilizing at a lower level years to decades later; however, interannual variability can continue. After 50 years of restoration of a temperate freshwater wetland and under comparable climatic conditions, Rocha and Goulden [2008] showed that vegetation dynamics strongly influenced the variability in annual cumulative NEE from a modest sink to a source.

The initial declines and continued variability observed in the annual wetland CO<sub>2</sub> uptake highlight the need for long-term continuous monitoring of restoration projects. The differences between years and study periods clearly show that sampling restored wetlands such as the one studied here for only 1 or 2 years will likely not provide an accurate assessment of long-term surface energy flux dynamics or GWP balance. This assessment is similar to that of Roulet *et al.* [2007], who noted that using any single year of a 6 year study to assess longer-term wetland carbon sequestration potential would result in errors as high as 4 times the annual flux. Whether a restored wetland becomes a net source or sink over longer periods of time depends on the

average of this considerable interannual variation, which is difficult to control or predict. Based on our observations in 2010–2011, even careful vegetation selection and water management did not lead to consistent annual CO<sub>2</sub> uptake.

## 5. Conclusion

Restoration of freshwater wetlands can enhance a multitude of ecosystem services, for example, expanding wildlife habitat, improving coastal protection in the face of sea level rise, and reducing atmospheric CO<sub>2</sub> through carbon sequestration. High rates of productivity and lower rates of remineralization in wetlands, such as those shown here, have stimulated interest in potentially using wetlands in biological carbon sequestration projects, perhaps leading to their use in emission reduction and trading programs. The concern this study highlights is that, while wetlands can sequester carbon in their soils, the interannual variability in CO<sub>2</sub> uptake, medium-term changes in wetland production, CH<sub>4</sub> emissions, and the effects of DOC export may make confident prediction or simple evaluation of the annual net GWP balance difficult. Indeed, our results show that intensive continuous monitoring is necessary for quantification of wetland carbon sequestration potential.

This study adds to the considerable evidence showing that reestablishment of wetlands initially results in high plant productivity and a net negative GWP balance, assuming the GWP of CH<sub>4</sub> is 34 times that of CO<sub>2</sub> for a 100 year time horizon. However, reduction in CO<sub>2</sub> uptake, observed here in 2010–2011, alters the overall carbon budget and GWP balance over time. Further, results of our study show that productivity can vary considerably between and among years, making evaluations of wetland performance difficult. Given the observed short- to medium-term variability for this wetland restoration project, it may be challenging to quantify net GWP reductions within the constraints of carbon offset and trading programs.

## Acknowledgments

Flux data from the restored wetland on Twitchell Island can be made available upon request. In the near future, we plan to make the data accessible through Ameriflux program (<http://ameriflux.ornl.gov>). This research was supported by the United States Geological Survey (USGS) Land Carbon Program, California's Department of Water Resources (DWR) Levee Program, and the USGS Cooperative Water Program. We specifically thank Curt Schmutte who helped conceive this wetland experiment. We are grateful for the independent USGS peer reviewers (Barclay Shoemaker) and anonymous journal reviewers for their valuable comments and edits. We would also like to recognize and thank John Franco Saraceno for his insightful discussions about uncertainty analysis and Matlab programing, as well as the many other scientists who have supported and advanced the science of this restored freshwater wetland over the past two decades. Any use of trade, firm, or product names is for descriptive purposes only and does not imply endorsement by the U.S. Government.

## References

- Aselmann, I., and P. J. Crutzen (1989), Global distribution of natural fresh-water wetlands and rice paddies, their net primary productivity, seasonality and possible methane emissions, *J. Atmos. Chem.*, 8(4), 307–358, doi:10.1007/bf00052709.
- Aubinet, M., T. Vesala, and D. Papale (Eds.) (2012), *Eddy Covariance: A Practical Guide to Measurement and Data Analysis*, Springer Science & Business Media, Netherlands.
- Aubrey, D. P., and R. O. Teskey (2009), Root-derived CO<sub>2</sub> efflux via xylem stream rivals soil CO<sub>2</sub> efflux, *New Phytol.*, 184(1), 35–40, doi:10.1111/j.1469-8137.2009.02971.x.
- Badiou, P., R. McDougal, D. Pennock, and B. Clark (2011), Greenhouse gas emissions and carbon sequestration potential in restored wetlands of the Canadian prairie pothole region, *Wetlands Ecol. Manage.*, 19(3), 237–256, doi:10.1007/s11273-011-9214-6.
- Baldocchi, D. D. (2003), Assessing the eddy covariance technique for evaluating carbon dioxide exchange rates of ecosystems: Past, present and future, *Global Change Biol.*, 9(4), 479–492, doi:10.1046/j.1365-2486.2003.00629.x.
- Bergamaschi, B. A., D. P. Krabbenhoft, G. R. Aiken, E. Patino, D. G. Rumbold, and W. H. Orem (2012), Tidally driven export of dissolved organic carbon, total mercury, and methylmercury from a mangrove-dominated estuary, *Environ. Sci. Technol.*, 46(3), 1371–1378, doi:10.1021/es2029137.
- Bloom, A. A., P. I. Palmer, A. Fraser, D. S. Reay, and C. Frankenberg (2010), Large-scale controls of methanogenesis inferred from methane and gravity spaceborne data, *Science*, 327(5963), 322–325, doi:10.1126/science.1175176.
- Bonn, A., et al. (2014), Investing in nature: Developing ecosystem service markets for peatland restoration, *Ecosyst. Serv.*, 9, 54–65, doi:10.1016/j.ecoser.2014.06.011.
- Bonneville, M.-C., I. B. Strachan, E. R. Humphreys, and N. T. Roulet (2008), Net ecosystem CO<sub>2</sub> exchange in a temperate cattail marsh in relation to biophysical properties, *Agric. For. Meteorol.*, 148(1), 69–81, doi:10.1016/j.agrformet.2007.09.004.
- Bossio, D. A., J. A. Fleck, K. M. Scow, and R. Fujii (2006), Alteration of soil microbial communities and water quality in restored wetlands, *Soil Biol. Biochem.*, 38(6), 1223–1233, doi:10.1016/j.soilbio.2005.09.027.
- Bridgman, S. D., J. P. Megonigal, J. K. Keller, N. B. Bliss, and C. Trettin (2006), The carbon balance of North American wetlands, *Wetlands*, 26(4), 889–916, doi:10.1672/0277-5212(2006)26[889:tcbona]2.0.co;2.
- Bridgman, S. D., H. Cadillo-Quiroz, J. K. Keller, and Q. Zhuang (2013), Methane emissions from wetlands: Biogeochemical, microbial, and modeling perspectives from local to global scales, *Global Change Biol.*, 19(5), 1325–1346, doi:10.1111/gcb.12131.
- Brix, H., B. K. Sorrell, and B. Lorenzen (2001), Are Phragmites-dominated wetlands a net source or net sink of greenhouse gases?, *Aquat. Bot.*, 69(2–4), 313–324, doi:10.1016/s0304-3770(01)00145-0.
- Bubier, J., P. Crill, A. Mosedale, S. Frolking, and E. Linder (2003), Peatland responses to varying interannual moisture conditions as measured by automatic CO<sub>2</sub> chambers, *Global Biogeochem. Cycles*, 17(2), 1066, doi:10.1029/2002GB001946.
- Burba, G. G., D. K. McDermitt, A. Grelle, D. J. Anderson, and L. K. Xu (2008), Addressing the influence of instrument surface heat exchange on the measurements of CO<sub>2</sub> flux from open-path gas analyzers, *Global Change Biol.*, 14(8), 1854–1876, doi:10.1111/j.1365-2486.2008.01606.x.
- Byrd, K. B., J. L. O'Connell, S. Di Tommaso, and M. Kelly (2014), Evaluation of sensor types and environmental controls on mapping biomass of coastal marsh emergent vegetation, *Remote Sens. Environ.*, 149, 166–180, doi:10.1016/j.rse.2014.04.003.
- Chanton, J. P., G. J. Whiting, J. D. Happell, and G. Gerard (1993), Contrasting rates and diurnal patterns of methane emission from emergent aquatic macrophytes, *Aquat. Bot.*, 46(2), 111–128, doi:10.1016/0304-3770(93)90040-4.
- Chu, H., J. Chen, J. F. Gottgens, Z. Ouyang, R. John, K. Czajkowski, and R. Becker (2014), Net ecosystem methane and carbon dioxide exchanges in a Lake Erie coastal marsh and a nearby cropland, *J. Geophys. Res. Biogeosci.*, 119, 722–740, doi:10.1002/2013JG002520.

- Chu, H., J. F. Gottgens, J. Chen, G. Sun, A. R. Desai, Z. Ouyang, C. Shao, and K. Czajkowski (2015), Climatic variability, hydrologic anomaly, and methane emission can turn productive freshwater marshes into net carbon sources, *Global Change Biol.*, 21(3), 1165–1181, doi:10.1111/gcb.12760.
- Craft, C., P. Megonigal, S. Broome, J. Stevenson, R. Freese, J. Cornell, L. Zheng, and J. Sacco (2003), The pace of ecosystem development of constructed *Spartina alterniflora* marshes, *Ecol. Appl.*, 13(5), 1417–1432, doi:10.1890/02-5086.
- Davidson, E. A., I. A. Janssens, and Y. Q. Luo (2006), On the variability of respiration in terrestrial ecosystems: Moving beyond Q(10), *Global Change Biol.*, 12(2), 154–164, doi:10.1111/j.1365-2486.2005.01065.x.
- Desai, A. R., et al. (2008), Cross-site evaluation of eddy covariance GPP and RE decomposition techniques, *Agric. For. Meteorol.*, 148(6–7), 821–838, doi:10.1016/j.agrformet.2007.11.012.
- Detto, M., J. Verfaillie, F. Anderson, L. Xu, and D. Baldocchi (2011), Comparing laser-based open- and closed-path gas analyzers to measure methane fluxes using the eddy covariance method, *Agric. For. Meteorol.*, 151(10), 1312–1324, doi:10.1016/j.agrformet.2011.05.014.
- Drexler, J. Z., C. S. de Fontaine, and T. A. Brown (2009a), Peat accretion histories during the past 6,000 years in marshes of the Sacramento-San Joaquin Delta, CA, USA, *Estuaries Coasts*, 32(5), 871–892, doi:10.1007/s12237-009-9202-8.
- Drexler, J. Z., C. S. de Fontaine, and S. J. Deverel (2009b), The legacy of wetland drainage on the remaining peat in the Sacramento-San Joaquin Delta, California, USA, *Wetlands*, 29(1), 372–386.
- Emmett-Mattox, S., S. Crooks, and J. Findsen (2010), Wetland grasses and gases: Are tidal wetlands ready for the carbon markets, *Natl. Wetlands Newsletter*, 32(6), 6–10.
- Euliss, N. H., R. A. Gleason, A. Olness, R. L. McDougal, H. R. Murkin, R. D. Robarts, R. A. Bourbonniere, and B. G. Warner (2006), North American prairie wetlands are important nonforested land-based carbon storage sites, *Sci. Total Environ.*, 361(1–3), 179–188, doi:10.1016/j.scitotenv.2005.06.007.
- Fleck, J. A., D. A. Bossio, and R. Fujii (2004), Dissolved organic carbon and disinfection by-product precursor release from managed peat soils, *J. Environ. Qual.*, 33(2), 465–475.
- Fleck, J. A., M. S. Fram, and R. Fujii (2007), Organic carbon and disinfection byproduct precursor loads from a constructed, non-tidal wetland in California's Sacramento-San Joaquin Delta, *San Francisco Estuary Watershed Sci.*, 5(2).
- Franssen, H. J. H., R. Stoeckli, I. Lehner, E. Rotenberg, and S. I. Seneviratne (2010), Energy balance closure of eddy-covariance data: A multisite analysis for European FLUXNET stations, *Agric. For. Meteorol.*, 150(12), 1553–1567, doi:10.1016/j.agrformet.2010.08.005.
- Galatowitsch, S. M. (2009), Carbon offsets as ecological restorations, *Restor. Ecol.*, 17(5), 563–570, doi:10.1111/j.1526-100X.2009.00587.x.
- Gamble, J. M., K. R. Burow, G. A. Wheeler, R. Hilditch, and J. Z. Drexler (2003), Hydrogeologic data from a shallow flooding demonstration project, Twitchell Island, California, 1997–2001, Report Rep. 2003–378.
- Garnet, K. N., J. P. Megonigal, C. Litchfield, and G. E. Taylor (2005), Physiological control of leaf methane emission from wetland plants, *Aquat. Bot.*, 81(2), 141–155, doi:10.1016/j.aquabot.2004.10.003.
- Goulden, M. L., M. Litvak, and S. D. Miller (2007), Factors that control *Typha* marsh evapotranspiration, *Aquat. Bot.*, 86(2), 97–106, doi:10.1016/j.aquabot.2006.09.005.
- Gu, L., W. M. Post, and A. W. King (2004), Fast labile carbon turnover obscures sensitivity of heterotrophic respiration from soil to temperature: A model analysis, *Global Biogeochem. Cycles*, 18, doi:10.1029/2003GB002119.
- Hahn-Schoffl, M., D. Zak, M. Minke, J. Gelbrecht, J. Augustin, and A. Freibauer (2011), Organic sediment formed during inundation of a degraded fen grassland emits large fluxes of CH<sub>4</sub> and CO<sub>2</sub>, *Biogeosciences*, 8(6), 1539–1550.
- Hatala, J. A., M. Detto, O. Sonnentag, S. J. Deverel, J. Verfaillie, and D. D. Baldocchi (2012), Greenhouse gas (CO<sub>2</sub>, CH<sub>4</sub>, H<sub>2</sub>O) fluxes from drained and flooded agricultural peatlands in the Sacramento-San Joaquin Delta, *Agric. Ecosyst. Environ.*, 150, 1–18, doi:10.1016/j.agee.2012.01.009.
- Herbst, M., T. Friberg, R. Ringgaard, and H. Soegaard (2011), Interpreting the variations in atmospheric methane fluxes observed above a restored wetland, *Agric. For. Meteorol.*, 151(7), 841–853, doi:10.1016/j.agrformet.2011.02.002.
- Kim, J., S. B. Verma, and D. P. Billesbach (1999), Seasonal variation in methane emission from a temperate Phragmites-dominated marsh: Effect of growth stage and plant-mediated transport, *Global Change Biol.*, 5(4), 433–440, doi:10.1046/j.1365-2486.1999.00237.x.
- Knox, S. H., C. Sturtevant, J. H. Matthes, L. Kottee, J. Verfaillie, and D. Baldocchi (2015), Agricultural peatland restoration: Effects of land-use change on greenhouse gas (CO<sub>2</sub> and CH<sub>4</sub>) fluxes in the Sacramento-San Joaquin Delta, *Global Change Biol.*, 21(2), 750–765, doi:10.1111/gcb.12745.
- Lafleur, P. M., N. T. Roulet, J. L. Bubier, S. Froking, and T. R. Moore (2003), Interannual variability in the peatland-atmosphere carbon dioxide exchange at an ombrotrophic bog, *Global Biogeochem. Cycles*, 17(2), 1036, doi:10.1029/2002GB001983.
- Malone, S. L., C. L. Staudhammer, H. W. Loescher, P. Olivas, S. F. Oberbauer, M. G. Ryan, J. Schedlbauer, and G. Starr (2014), Seasonal patterns in energy partitioning of two freshwater marsh ecosystems in the Florida Everglades, *J. Geophys. Res. Biogeosci.*, 119, 1487–1505, doi:10.1002/2014JG002700.
- Miller, R. L. (2011), Carbon gas fluxes in re-established wetlands on organic soils differ relative to plant community and hydrology, *Wetlands*, 31(6), 1055–1066, doi:10.1007/s13157-011-0215-2.
- Miller, R. L., and R. Fujii (2010), Plant community, primary productivity, and environmental conditions following wetland re-establishment in the Sacramento-San Joaquin Delta, California, *Wetlands Ecol. Manage.*, 18(1), 1–16, doi:10.1007/s11273-009-9143-9.
- Miller, R. L., M. Fram, R. Fujii, and G. Wheeler (2008), Subsidence reversal in a re-established wetland in the Sacramento-San Joaquin Delta, California, USA, *San Francisco Estuary Watershed Sci.*, 6(3).
- Mitra, S., R. Wassmann, and P. L. G. Vlek (2005), An appraisal of global wetland area and its organic carbon stock, *Curr. Sci.*, 88(1), 25–35.
- Mitsch, W. J., B. Bernal, A. M. Nahlik, U. Mander, L. Zhang, C. J. Anderson, S. E. Jorgensen, and H. Brix (2013), Wetlands, carbon, and climate change, *Landscape Ecol.*, 28(4), 583–597, doi:10.1007/s10980-012-9758-8.
- Moffat, A. M., et al. (2007), Comprehensive comparison of gap-filling techniques for eddy covariance net carbon fluxes, *Agric. For. Meteorol.*, 147(3–4), 209–232, doi:10.1016/j.agrformet.2007.08.011.
- Mount, J., and R. Twiss (2005), Subsidence, sea level rise, and seismicity in the Sacramento-San Joaquin Delta, *San Francisco Estuary Watershed Sci.*, 3(1).
- Myhre, G., D. Shindell, F. Bréon, W. Collins, J. Fuglestvedt, J. Huang, D. Koch, J. Lamarque, D. Lee, and B. Mendoza (2013), Anthropogenic and natural radiative forcing, in *Climate Change 2013: The Physical Science Basis. Contribution of Working Group I to the Fifth Assessment Report of the Intergovernmental Panel on Climate Change*, edited by T. F. Stocker, et al., Chap. 8, Cambridge Univ. Press, Cambridge, U. K., and New York.
- Neubauer, S. C. (2014), On the challenges of modeling the net radiative forcing of wetlands: Reconsidering Mitsch et al. 2013, *Landscape Ecol.*, 29(4), 571–577, doi:10.1007/s10980-014-9986-1.
- Neubauer, S. C., and J. P. Megonigal (2015), Moving beyond global warming potentials to quantify the climatic role of ecosystems, *Ecosystems*, 18(6), 1000–1013, doi:10.1007/s10021-015-9879-4.

- Olson, D. M., T. J. Griffis, A. Noormets, R. Kolka, and J. Chen (2013), Interannual, seasonal, and retrospective analysis of the methane and carbon dioxide budgets of a temperate peatland, *J. Geophys. Res. Biogeosci.*, 118, 226–238, doi:10.1002/jgrg.20031.
- Papale, D., and A. Valentini (2003), A new assessment of European forests carbon exchanges by eddy fluxes and artificial neural network spatialization, *Global Change Biol.*, 9(4), 525–535, doi:10.1046/j.1365-2486.2003.00609.x.
- Petrescu, A. M. R., et al. (2015), The uncertain climate footprint of wetlands under human pressure, *Proc. Natl. Acad. Sci. U.S.A.*, 112(15), 4594–4599, doi:10.1073/pnas.1416267112.
- Reichstein, M., et al. (2005), On the separation of net ecosystem exchange into assimilation and ecosystem respiration: Review and improved algorithm, *Global Change Biol.*, 11(9), 1424–1439, doi:10.1111/j.1365-2486.2005.001002.x.
- Richardson, A. D., and D. Y. Hollinger (2005), Statistical modeling of ecosystem respiration using eddy covariance data: Maximum likelihood parameter estimation, and Monte Carlo simulation of model and parameter uncertainty, applied to three simple models, *Agric. For. Meteorol.*, 131(3–4), 191–208, doi:10.1016/j.agrformet.2005.05.008.
- Richardson, A. D., and D. Y. Hollinger (2007), A method to estimate the additional uncertainty in gap-filled NEE resulting from long gaps in the CO<sub>2</sub> flux record, *Agric. For. Meteorol.*, 147(3–4), 199–208, doi:10.1016/j.agrformet.2007.06.004.
- Richardson, A. D., M. D. Mahecha, E. Falge, J. Kattge, A. M. Moffat, D. Papale, M. Reichstein, V. J. Stauch, B. H. Braswell, and G. Churkina (2008), Statistical properties of random CO<sub>2</sub> flux measurement uncertainty inferred from model residuals, *Agric. For. Meteorol.*, 148(1), 38–50.
- Richardson, C. J. (2010), The Everglades: North America's subtropical wetland, *Wetlands Ecol. Manage.*, 18(5), 517–542, doi:10.1007/s11273-009-9156-4.
- Rippke, M. B., M. T. Distler, and J. M. Farrell (2010), Holocene vegetation dynamics of an upper St. Lawrence River wetland: Paleoecological evidence for a recent increase in Cattail (*Typha*), *Wetlands*, 30(4), 805–816, doi:10.1007/s13157-010-0068-0.
- Rocha, A. V., and M. L. Goulden (2008), Large interannual CO<sub>2</sub> and energy exchange variability in a freshwater marsh under consistent environmental conditions, *J. Geophys. Res.*, 113, G04019, doi:10.1029/2008JG000712.
- Rocha, A. V., and M. L. Goulden (2009), Why is marsh productivity so high? New insights from eddy covariance and biomass measurements in a *Typha* marsh, *Agric. For. Meteorol.*, 149(1), 159–168, doi:10.1016/j.agrformet.2008.07.010.
- Roulet, N. T., P. M. Lafleur, P. J. H. Richard, T. R. Moore, E. R. Humphreys, and J. Bubier (2007), Contemporary carbon balance and late Holocene carbon accumulation in a northern peatland, *Global Change Biol.*, 13(2), 397–411, doi:10.1111/j.1365-2486.2006.01292.x.
- Savage, K. E., and E. A. Davidson (2001), Interannual variation of soil respiration in two New England forests, *Global Biogeochem. Cycles*, 15(2), 337–350, doi:10.1029/1999GB001248.
- Schedlbauer, J. L., J. W. Munyon, S. F. Oberbauer, E. E. Gaiser, and G. Starr (2012), Controls on ecosystem carbon dioxide exchange in short- and long-hydroperiod Florida Everglades freshwater marshes, *Wetlands*, 32(5), 801–812, doi:10.1007/s13157-012-0311-y.
- Schile, L. M., K. B. Byrd, L. Windham-Myers, and M. Kelly (2013), Accounting for non-photosynthetic vegetation in remote-sensing-based estimates of carbon flux in wetlands, *Remote Sens. Lett.*, 4(6), 542–551, doi:10.1080/2150704x.2013.766372.
- Schröer-Uijl, A. P., P. S. Kroon, D. M. D. Hendriks, A. Hensen, J. Van Huissteden, F. Berendse, and E. M. Veenendaal (2014), Agricultural peatlands: Towards a greenhouse gas sink—A synthesis of a Dutch landscape study, *Biogeosciences*, 11(16), 4559–4576, doi:10.5194/bg-11-4559-2014.
- Stoy, P. C., et al. (2013), A data-driven analysis of energy balance closure across FLUXNET research sites: The role of landscape scale heterogeneity, *Agric. For. Meteorol.*, 171, 137–152, doi:10.1016/j.agrformet.2012.11.004.
- Sturtevant, C., B. L. Ruddell, S. H. Knox, J. Verfaillie, J. H. Matthes, P. Y. Oikawa, and D. Baldocchi (2016), Identifying scale-emergent, non-linear, asynchronous processes of wetland methane exchange, *J. Geophys. Res. Biogeosci.*, 121, 188–204, doi:10.1002/2015JG003054.
- Thompson, J. (1957), Sacramento-San Joaquin Delta, California, Stanford Univ.
- Waddington, J. M., M. Strack, and M. J. Greenwood (2010), Toward restoring the net carbon sink function of degraded peatlands: Short-term response in CO<sub>2</sub> exchange to ecosystem-scale restoration, *J. Geophys. Res.*, 115, G01008, doi:10.1029/2009JG001090.
- Webb, E., G. Pearman, and R. Leuning (1980), Correction of flux measurements for density effects due to heat and water vapour transfer, *Q. J. R. Meteorol. Soc.*, 106(447), 85–100.
- Whiting, G. J., and J. P. Chanton (1993), Primary production control of methane emission from wetlands, *Nature*, 364(6440), 794–795, doi:10.1038/364794a0.
- Whiting, G. J., and J. P. Chanton (2001), Greenhouse carbon balance of wetlands: Methane emission versus carbon sequestration, *Tellus Ser. B-Chem. Phys. Meteorol.*, 53(5), 521–528, doi:10.1034/j.1600-0889.2001.530501.x.
- Wilson, K., et al. (2002), Energy balance closure at FLUXNET sites, *Agric. For. Meteorol.*, 113(1–4), 223–243, doi:10.1016/s0168-1923(02)00109-0.